

Perspective: Intraband divergences in third order optical response of 2D systems

J. L. Cheng,^{1, 2, a)} J. E. Sipe,^{3, b)} S. W. Wu,^{4, c)} and Chunlei Guo^{1, 5, d)}

¹⁾*The Guo China-US Photonics Laboratory, Changchun Institute of Optics, Fine Mechanics and Physics, Chinese Academy of Sciences, 3888 Eastern South Lake Road, Changchun, Jilin 130033, China.*

²⁾*University of Chinese Academy of Sciences, Beijing 100049, China*

³⁾*Department of Physics and Institute for Optical Sciences, University of Toronto, 60 St. George Street, Toronto, Ontario M5S 1A7, Canada*

⁴⁾*State Key Laboratory of Surface Physics, Key Laboratory of Micro and Nano Photonic Structures (MOE), and Department of Physics, Fudan University, Shanghai 200433, China*

⁵⁾*The Institute of Optics, University of Rochester, Rochester, NY 14627, USA.*

The existence of large nonlinear optical coefficients is one of the preconditions for using nonlinear optical materials in nonlinear optical devices. For a crystal, such large coefficients can be achieved by matching photon energies with resonant energies between different bands, and so the details of the crystal band structure play an important role. Here we demonstrate that large third-order nonlinearities can also be generally obtained by a different strategy: As any of the incident frequencies or the sum of any two or three frequencies approaches zero, the doped or excited populations of electronic states lead to divergent contributions in the induced current density. We refer to these as intraband divergences, by analogy with the behavior of Drude conductivity in linear response. Physically, such resonant processes can be associated with a combination of intraband and interband optical transitions. Current-induced second order nonlinearity, coherent current injection, and jerk currents are all related to such divergences, and we find similar divergences in degenerate four wave mixing and cross-phase modulation under certain conditions. These divergences are limited by intraband relaxation parameters, and lead to a large optical response from a high quality sample; we find they are very robust with respect to variations in the details of the band structure. To clearly track all of these effects, we analyze gapped graphene, describing the electrons as massive Dirac fermions; under the relaxation time approximation, we derive analytic expressions for the third order conductivities, and identify the divergences that arise in describing the associated nonlinear phenomena.

^{a)}Electronic mail: jlcheng@ciomp.ac.cn

^{b)}Electronic mail: sipe@physics.utoronto.ca

^{c)}Electronic mail: swwu@fudan.edu.cn

^{d)}Electronic mail: chunlei.guo@rochester.edu

I. INTRODUCTION

Motivated by the novel optical properties of graphene,¹⁻³ many researchers have turned their attention to the linear and nonlinear optical response of 2D systems more generally.^{4,5} While there are certainly strong-field excitation circumstances under which a perturbative treatment will fail,⁶⁻⁹ for many materials a useful first step towards understanding the optical response is the calculation of the conductivities that arise in an expansion of the response of the induced current density in powers of the electric field.¹⁰ In materials where inversion symmetry is present, or its lack can be neglected, the first non-vanishing nonlinear response coefficient in the long-wavelength limit arises at third order, and that is our focus in this paper. The simplest approach one can take to calculate such response coefficients is to treat the electrons in an independent particle approximation,¹¹ describing any electron-electron scattering effects and interactions with phonons by the introduction of phenomenological relaxation rates. Such a strategy certainly has its limitations, but at least it identifies many of the qualitative features of the optical response, and in particular it identifies what we call “divergences” in that response. We use this term to refer to the infinite optical response coefficients that are predicted at certain frequencies or sets of frequencies in the so-called “clean limit,” where all scattering effects, including carrier-carrier scattering, carrier-phonon scattering, and carrier-impurity scattering, are ignored by omitting any relaxation rates from the calculation. Under these conditions the actual predicted magnitude of a response depends critically on the values chosen for the phenomenological relaxation rates. These “divergences” are of particular interest to experimentalists because they indicate situations where the optical response can be expected to be large; they are also of particular interest to theorists since they indicate conditions under which a more sophisticated treatment of scattering within the material, or perhaps a treatment of the response more sophisticated than the perturbative one, is clearly in order.

The optical response of a crystal arises due to interband and intraband transitions.¹¹ Resonances can be associated with both transitions. For linear optical response, only a single optical transition is involved. A single interband transition can be on resonance for a large range of photon energies, as long as the photon energy is above the band gap. But the resonant electronic states are limited to those with the energy difference matching the photon energy, which depend on the details of the band structure. A single intraband

transition can be on resonance only for zero photon energy, and for electronic states at the Fermi surface. Thus, whether or not these resonances lead to a divergent optical response can depend strongly on the material being considered. For the nonlinear optical response, intraband and interband transitions can be combined, leading to complicated nonlinear optical transitions.^{12,13} As with single intraband transitions, when the nonlinear optical transitions involve the same initial and final electronic states the resonant frequency, which is the sum of all involved frequencies, is also zero. This is analogous to the Drude conductivity in linear response, which diverges at zero frequency in the “clean limit.” However, due to the interplay of interband transitions, the incident frequencies need not necessarily all be zero for there to be a divergence, and the involved electronic states need not necessarily be around the Fermi surface. By explicitly deriving the general expressions for the third order nonlinear conductivities in the clean limit, we show that the existence and characteristics of such divergences are of a more general nature. To highlight them in a clear and tractable way, we apply our approach to 2D gapped graphene, for which the perturbative third order conductivities can be analytically obtained from the Dirac-like band structure in the single particle approximation. Although our discussion is in the context of such 2D systems, the underlying physics is the same for systems of different dimension.

Because the nonlinear transitions involve a number of frequencies, these divergences can be classified into different types, associated with different types of nonlinear phenomena. Several of these have been widely studied in the literature, usually within the context of a particular material or model or excitation condition; yet the connection with the general nonlinear conductivities is seldom discussed. Our goal here is to demonstrate the general nature of the expressions for the response across a range of materials.

The first type of divergence can be called “current-induced second order nonlinearity” (CISNL). It arises when free electrons in the system are driven by an applied DC field; the induced DC current breaks the initial inversion symmetry, and thus the material exhibits an effective second-order response to applied optical fields, leading to phenomena such as sum and difference frequency generation. The nature of the divergence here is in the response to the DC field, similar to a single intraband resonance, which would be infinite if phenomenological relaxation terms were not introduced; however, when written as proportional to the induced DC current, the effective second-order response coefficients are finite. This phenomenon has been investigated extensively in different materials, both

experimentally^{14–18} and theoretically^{19–21}. A second type is “coherent current injection” (CCI),^{22–24} where the presence of fields at ω and $2\omega - \delta$ leads to a divergent DC response as $\delta \rightarrow 0$ if the excitation at 2ω is able to create free carriers; the divergent response signals the injection of current by the interference of one-photon absorption and degenerate two-photon absorption amplitudes. This is the most widely studied process, both experimentally^{25,26} and theoretically.^{27–30} Recent theoretical work has also identified an injection process associated with one-photon absorption and the stimulated Raman process.^{28,31} A third type is the jerk current,^{32,33} which is a new type of one color CCI with the assistance of a static electric field. It is a high order divergence involving both a static electric field and an optical field. The static DC field can change the carrier injection rate induced by the optical field, as well as a hydrodynamic acceleration of these optically injected carriers; thus, as opposed to the usual two-color CCI, the injection rate of the jerk current increases with the injection time.

We can also identify new divergences, which have not been well recognized in the literature, for two familiar third order nonlinear phenomena. The first arises in cross-phase modulation (XPM) when fields at ω_p and ω_s are present. The response for the field at ω_s due to the field at ω_p can diverge when ω_p is above or near the energy gap, leading to a phase modulation of the field at ω_s that is limited by a relaxation rate. The second also involves excitation with fields at ω_p and ω_s , but focuses on the degenerate four-wave mixing (DFWM) field generated at $2\omega_p - \omega_s$. As $\omega_s \rightarrow \omega_p$ this term diverges for ω_p above or near the energy gap. These cases merge as $\omega_p \rightarrow \omega_s$, which corresponds to the most widely studied nonlinear phenomenon of Kerr effects and two-photon absorption.^{34–42} The very large variation of the extracted values of the nonlinear susceptibilities associated with these phenomena^{5,41,43} may be related to such divergences.

In section II we review the general expressions for the third order optical response in the independent particle approximation, and identify in general the divergences that appear associated with the nonlinear optical transitions with a vanishing total frequency. In section III we specialize to the case of gapped graphene, and use it as an example to illustrate the divergences. In section IV we point out the differences between the divergent behavior of gapped and ungapped graphene. In section V we conclude.

II. THE THIRD ORDER RESPONSE CONDUCTIVITIES

The general third order nonlinear susceptibility have been well studied in the literature for a cold intrinsic semiconductor,¹¹ with a large effort devoted to working out many subtle features. In this section we mainly repeat the same procedure for a general band system, and classify the expression in a way that the divergent term can be easily identified.

Writing the electric field $\mathbf{E}(t)$ as

$$\mathbf{E}(t) = \sum_i \mathbf{E}(\omega_i) e^{-i\omega t}, \quad (1)$$

and other fields similarly, to third order in the electric field the induced current density $\mathbf{J}^{(3)}(t)$ is characterized by the response coefficients $\sigma^{(3);dabc}(\omega_1, \omega_2, \omega_3)$,

$$J^{(3);d}(\omega_1 + \omega_2 + \omega_3) = \sum_{\omega_1, \omega_2, \omega_3} \sigma^{(3);dabc}(\omega_1, \omega_2, \omega_3) E^a(\omega_1) E^b(\omega_2) E^c(\omega_3) \quad (2)$$

where superscripts a, b, \dots indicate Cartesian components and are summed over when repeated. The coefficients $\sigma^{(3);abcd}(\omega_1, \omega_2, \omega_3)$ can be taken to be symmetric under simultaneous permutation of (bcd) and $(\omega_1, \omega_2, \omega_3)$, and since the sums over the ω_i are over all frequencies there are “degeneracy factors” that arises under certain combinations of frequencies. For example, if fields at ω_p and ω_s are present we have

$$J^d(2\omega_p - \omega_s) = 3\sigma^{(3);dabc}(\omega_p, \omega_p, -\omega_s) E^a(\omega_p) E^b(\omega_p) E^c(-\omega_s). \quad (3)$$

Often the response coefficient $\sigma^{(3);dabc}(\omega_1, \omega_2, \omega_3)$ is written as $\sigma^{(3);dabc}(-\omega_1 - \omega_2 - \omega_3; \omega_1, \omega_2, \omega_3)$. We do not do that here to avoid cluttering the notation, but we consider it implicit in that when we picture these response coefficients we draw arrows associated with all four of the variables appearing in $\sigma^{(3);dabc}(-\omega_1 - \omega_2 - \omega_3; \omega_1, \omega_2, \omega_3)$, upward arrows associated with positive variables and downward arrows associated with negative variables.

To calculate the response coefficients in the independent particle approximation we label the bands by lower case letters n, m , etc., and the wave vectors in the first Brillouin zone by \mathbf{k} . The density operator elements $\rho_{nm\mathbf{k}}$ associated with bands n, m and wave vector \mathbf{k}

satisfy the equation of motion¹¹

$$\begin{aligned}
i\hbar \frac{\partial \rho_{nm\mathbf{k}}(t)}{\partial t} &= (\varepsilon_{n\mathbf{k}} - \varepsilon_{m\mathbf{k}}) \rho_{nm\mathbf{k}} - e\mathbf{E}(t) \cdot \left[\sum_{l \neq n} \boldsymbol{\xi}_{nl\mathbf{k}} \rho_{lm\mathbf{k}}(t) - \sum_{l \neq m} \rho_{nl\mathbf{k}}(t) \boldsymbol{\xi}_{lm\mathbf{k}} \right] \\
&\quad - ie\mathbf{E}(t) \cdot [\nabla_{\mathbf{k}} \rho_{nm\mathbf{k}}(t) - i(\boldsymbol{\xi}_{n\mathbf{k}} - \boldsymbol{\xi}_{m\mathbf{k}}) \rho_{nm\mathbf{k}}(t)] \\
&\quad + i\hbar \left. \frac{\partial \rho_{nm\mathbf{k}}}{\partial t} \right|_{\text{scat}}. \tag{4}
\end{aligned}$$

Here we describe the interaction of light with the matter using the “ $\mathbf{r} \cdot \mathbf{E}$ ” approach rather than the “ $\mathbf{p} \cdot \mathbf{A}$ ” approach involving the vector potential $\mathbf{A}(t)$, for the latter can lead to false divergences associated with the violation of sum rules when the number of bands are inevitably truncated to make any calculation. The coefficients $\boldsymbol{\xi}_{nm\mathbf{k}}$ are the Berry connections, using the definition in the work by Aversa and Sipe.¹¹ The interband optical transitions are identified by the off-diagonal terms of $\boldsymbol{\xi}_{nm\mathbf{k}}$, while the rest of terms associated with $\mathbf{E}(t)$ are associated with the intraband optical transitions. The last term, $i\hbar \left. \frac{\partial \rho_{nm\mathbf{k}}}{\partial t} \right|_{\text{scat}}$, describes the relaxation processes. In our approach, we take a relaxation time approximation, and specify different relaxation time for different transitions, as given below. We solve Eq. (4) perturbatively by setting $\rho(t) = \sum_{j \geq 0} \rho^{(j)}(t)$, where $\rho^{(0)}(t) = \rho^0$ stands for the density matrix in the thermal equilibrium, and $\rho^{(j)}(t) \propto [\mathbf{E}]^j$. The iteration for each order is given by

$$\begin{aligned}
i\hbar \frac{\partial \rho_{nm\mathbf{k}}^{(j+1)}(t)}{\partial t} &= (\varepsilon_{n\mathbf{k}} - \varepsilon_{m\mathbf{k}}) \rho_{nm\mathbf{k}}^{(j+1)} - e\mathbf{E}(t) \cdot \left[\sum_{l \neq n} \boldsymbol{\xi}_{nl\mathbf{k}} \rho_{lm\mathbf{k}}^{(j)}(t) - \sum_{l \neq m} \rho_{nl\mathbf{k}}^{(j)}(t) \boldsymbol{\xi}_{lm\mathbf{k}} \right] \\
&\quad - ie\mathbf{E}(t) \cdot \left[\nabla_{\mathbf{k}} \rho_{nm\mathbf{k}}^{(j)}(t) - i(\boldsymbol{\xi}_{n\mathbf{k}} - \boldsymbol{\xi}_{m\mathbf{k}}) \rho_{nm\mathbf{k}}^{(j)}(t) \right] + i\hbar \left. \frac{\partial \rho_{nm\mathbf{k}}^{(j+1)}}{\partial t} \right|_{\text{scat}}, \tag{5}
\end{aligned}$$

where we take the relaxation terms⁴⁴ as

$$\left. \hbar \frac{\partial \rho_{nn\mathbf{k}}^{(j)}}{\partial t} \right|_{\text{scat}} = -\Gamma_a^{(j)} \rho_{nn\mathbf{k}}^{(j)}, \tag{6}$$

$$\left. \hbar \frac{\partial \rho_{nm\mathbf{k}}^{(j)}}{\partial t} \right|_{\text{scat}} = -\Gamma_e^{(j)} \rho_{nm\mathbf{k}}^{(j)}, \text{ for } n \neq m. \tag{7}$$

Here the $\Gamma_e^{(j)}$ and $\Gamma_a^{(j)}$ are phenomenological relaxation parameters associated with interband and intraband motion respectively, with the superscript (j) indicating the order of perturbation at which they are introduced. At optical frequencies, the presence of relaxation parameters removes divergences associated with the resonances, and the values of the relaxation parameters are important for evaluating the nonlinear conductivities when

resonant transitions exist. It is natural to choose different values of $\Gamma_{e/a}^{(j)}$ for resonant and non-resonant transitions. A general perturbative solution are presented in Appendix A.

With the evolution of the density matrix, the current density can be obtained through $\mathbf{J}(t) = e \sum_{nm} \int \frac{d\mathbf{k}}{(2\pi)^2} \mathbf{v}_{mn\mathbf{k}} \rho_{nm\mathbf{k}}(t)$, where $\mathbf{v}_{mn\mathbf{k}}$ are the matrix elements for a velocity operator. A third order response calculation¹⁰ leads to the result

$$\begin{aligned} \sigma^{(3);dabc}(\omega_1, \omega_2, \omega_3) = & \frac{1}{6} \left[\tilde{\sigma}^{(3);dabc}(\omega, \omega_2 + \omega_3, \omega_3) + \tilde{\sigma}^{(3);dacb}(\omega, \omega_2 + \omega_3, \omega_2) \right. \\ & + \tilde{\sigma}^{(3);dbac}(\omega, \omega_1 + \omega_3, \omega_3) + \tilde{\sigma}^{(3);dbca}(\omega, \omega_1 + \omega_3, \omega_1) \\ & \left. + \tilde{\sigma}^{(3);dcba}(\omega, \omega_1 + \omega_2, \omega_1) + \tilde{\sigma}^{(3);dcab}(\omega, \omega_1 + \omega_2, \omega_2) \right], \end{aligned} \quad (8)$$

with $\omega = \omega_1 + \omega_2 + \omega_3$, and the unsymmetrized coefficients $\tilde{\sigma}^{(3);dabc}(\omega, \omega_0, \omega_3)$ take the form

$$\begin{aligned} \tilde{\sigma}^{(3);dabc}(\omega, \omega_0, \omega_3) = & \frac{1}{vv_0v_3} S_1^{dabc} + \frac{1}{vv_0} S_2^{dabc}(w_3) + \frac{1}{vv_3} S_3^{dabc}(w_0) + \frac{1}{v} S_4^{dabc}(w_0, w_3) \\ & + \frac{1}{v_0v_3} S_5^{dabc}(w) + \frac{1}{v_0} S_6^{dabc}(w, w_3) + \frac{1}{v_3} S_7^{dabc}(w, w_0) + S_8^{dabc}(w, w_0, w_3) \end{aligned} \quad (9)$$

with

$$v = \hbar\omega + i\Gamma_a^{(3)}, \quad w = \hbar\omega + i\Gamma_e^{(3)}, \quad (10)$$

$$v_0 = \hbar\omega_0 + i\Gamma_a^{(2)}, \quad w_0 = \hbar\omega_0 + i\Gamma_e^{(2)}, \quad (11)$$

$$v_3 = \hbar\omega_3 + i\Gamma_a^{(1)}, \quad w_3 = \hbar\omega_3 + i\Gamma_e^{(1)}. \quad (12)$$

Note that the actual value of the energy appearing in, for example, v_0 depends on the corresponding frequency (here ω_0 , a sum of two of the incident frequencies) appearing in $\tilde{\sigma}^{(3);dabc}(\omega, \omega_0, \omega_3)$. The quantities v , v_0 , and v_3 are associated with the intraband motions (for carriers or excited carriers). The coefficients S_i^{dabc} are associated with interband transitions; we give expressions for them, and for the expressions to which they reduce for the particular models we consider, in the Appendix B. Any divergences they contain are associated with interband motion, and thus all the intraband divergences are explicitly indicated by the v_i in the denominators appearing in Eq. (9). Thus it is the $\Gamma_a^{(i)}$ that will be of importance to us. Typically one $\Gamma_a^{(i)}$ is important for a given divergence; the other $\Gamma_a^{(j)}$, and the $\Gamma_e^{(j)}$, to which the process is not sensitive, are all set equal to a nominal value Γ . These divergent processes are summarized in Table I.

The general expression for the conductivity in Eq. (9) immediately indicates the possibilities of the nonlinear phenomena discussed in the Introduction. For CISNL, the conductivities

	$v_3 \sim 0$	$v_0 \sim 0$	$v \sim 0$
Conductivity	$\sigma^{(3)}(\omega_1, \omega_2, \delta)$	$\sigma^{(3)}(\omega_1, \omega, -\omega + \delta)$	$\sigma^{(3)}(\omega_1, \omega_2, -\omega_1 - \omega_2 + \delta)$
Divergence	$[\hbar\delta + i\Gamma_a^{(1)}]^{-1}$	$[\hbar\delta + i\Gamma_a^{(2)}]^{-1}$	$[\hbar\delta + i\Gamma_a^{(3)}]^{-1}$
Nonlinear phenomena	CISNL jerk current	XPM, DFWM jerk current	CCI
Divergent contributions			
Resonant conditions	doped	$\hbar\omega > 2E_c$	(left) $\hbar\omega_1 > 2E_c$ (right) $\hbar\omega_1 + \hbar\omega_2 > 2E_c$

TABLE I. Illustration of the resonant processes of the divergences associated with the intraband motion. The row “Divergent contributions” illustrates the divergent transitions, by the magenta arrows and labels in the diagram. The magenta dots show the doped or excited electronic states. The row “Resonant conditions” gives the conditions for these resonances.

$\sigma^{(3);dabc}(\omega_1, \omega_2, 0)$ include divergences associated with $v_3 \rightarrow 0$; for coherent current injection, the conductivities $\sigma^{(3);dabc}(-2\omega, \omega, \omega)$ include divergences associated with $v \rightarrow 0$; the jerk current is a special case of CISNL, described by $\sigma^{(3);dabc}(\omega, -\omega, 0)$, with divergences associated with $v_3 \rightarrow 0$ and $v \rightarrow 0$; for XPM and DFWM, the conductivities $\sigma^{(3);dabc}(\omega, \omega_p, -\omega_p)$ and $\sigma^{(3);dabc}(-\omega_s, \omega_p, \omega_p)$ include divergences associated with $v_0 \rightarrow 0$. In special cases, there may be extra divergences identified by a combination of these limits, and the detailed divergences types are determined by the values of S_i . Of course, for finite relaxation times we will not have a vanishing v_3 , v_0 , or v . Nonetheless, for frequencies where the real part of one of these quantities vanishes the term(s) in Eq. (9) containing this quantity will make the largest contribution, and we refer to them as the “divergent contributions.” Our focus is the identification of these divergent contributions. Before getting into the details of these effects, it is helpful to isolate the divergent contributions in these conductivities, as shown in Table II.

Nonlinear phenomenon	conductivity	Condition for nonzero A_i	Note/Reference
CISNL	$\sigma^{(3)}(\omega_1, \omega_2, 0) \rightarrow \frac{1}{\Gamma_a^{(1)}} A_1 + B_1$	doped	A_1 : CISHG ^{19–21,44}
			B_1 : EFISH ⁴⁴
XPM	$\sigma^{(3)}(\omega_s, \omega_p, -\omega_p) \rightarrow \frac{1}{\Gamma_a^{(2)}} A_1 + B_1$	$\hbar\omega_p \geq 2E_c$	
DFWM*	$\sigma^{(3)}(\omega_p, \omega_p, -\omega_s) \rightarrow \frac{1}{\Gamma_a^{(2)}} \left(\frac{1}{\Gamma} A_1 + A_2 \right) + B_1$	$\hbar\omega_p \geq 2E_c$	$\omega_s \sim \omega_p$ B_1 : Kerr effects, ⁴⁴ TPA
CCI	$\sigma^{(3)}(\omega, \omega, -2\omega) \rightarrow \frac{1}{\Gamma_a^{(3)}} (A_1 + A_2) + B_1$	A_1 : $\hbar\omega > E_c$	usual CCI ^{22–30}
		A_2 : $\hbar\omega > 2E_c$	stimulated Raman process ^{28,31}
Jerk current	$\sigma^{(3)}(\omega, -\omega, 0) \rightarrow \frac{1}{\Gamma_a^{(3)}} \left(\frac{1}{\Gamma_a^{(2)}} A_1 + \frac{1}{\Gamma_a^{(1)}} A_2 + A_3 \right) + B_1$	A_1 : $\hbar\omega > 2E_c$	^{32,33}
		A_2 : doped	

TABLE II. A short summary of the structure of the divergences in the nonlinear optical phenomena discussed in this work. Here $2E_c$ is the gap or the chemical potential induced gap; all the A_i and B_i are expansion coefficients. The third column lists the condition when the divergences can occur. (*) Here we set all the relaxation parameters $\Gamma_{a/e}^{(j)}$ except $\Gamma_a^{(2)}$ equal to Γ .

III. NONLINEAR OPTICAL CONDUCTIVITY OF GAPPED GRAPHENE

We apply the approach to gapped graphene, a two dimensional system. The low energy excitations exist in two valleys, which can be described by a simplified two band model for the unperturbed Hamiltonian

$$H_{\tau\mathbf{k}}^0(\Delta) = \begin{pmatrix} \Delta & \hbar v_F (ik_x + \tau k_y) \\ \hbar v_F (-ik_x + \tau k_y) & -\Delta \end{pmatrix}. \quad (13)$$

The quantity $\mathbf{k} = k_x \hat{\mathbf{x}} + k_y \hat{\mathbf{y}}$ is a two dimensional wave vector, $\Delta \geq 0$ is a mass parameter to induce a band gap 2Δ , $\tau = \pm$ stands for a valley index, and v_F is the Fermi velocity. Ungapped graphene corresponds to the limit $\Delta \rightarrow 0$. All the necessary quantities for the

calculation of the third order conductivity are given⁴⁵ by

$$\varepsilon_{\tau s \mathbf{k}} = s \epsilon_k, \text{ with } \epsilon_k = \sqrt{(\hbar v_F k)^2 + \Delta^2}, \quad (14a)$$

$$\boldsymbol{\xi}_{\tau+-\mathbf{k}} = \frac{\hbar v_F (i k_x + \tau k_y)}{2 \epsilon_k k^2} \left(-i \frac{\Delta}{\epsilon_k} \mathbf{k} + \tau \mathbf{k} \times \hat{\mathbf{z}} \right), \quad (14b)$$

$$\boldsymbol{\xi}_{\tau++\mathbf{k}} - \boldsymbol{\xi}_{\tau--\mathbf{k}} = \frac{1}{k^2} \left(1 - \frac{\Delta}{\epsilon_k} \right) \tau \mathbf{k} \times \hat{\mathbf{z}}, \quad (14c)$$

$$\mathbf{v}_{\tau+-\mathbf{k}} = 2i \hbar^{-1} \epsilon_k \boldsymbol{\xi}_{\tau+-\mathbf{k}}, \quad (14d)$$

$$\mathbf{v}_{\tau s s \mathbf{k}} = \hbar^{-1} \nabla_{\mathbf{k}} \varepsilon_{\tau s \mathbf{k}}. \quad (14e)$$

For the special two band system we use $s = \pm$ to indicate the upper (+) and lower (-) bands.

In this approximation for the dispersion relation of the bands, all the S_j^{dabc} can be analytically obtained, and are listed in Appendix B. Furthermore, the unsymmetrized conductivity $\tilde{\sigma}^{(3);dabc}(\omega, \omega_0, \omega_3)$ can be written as the sum of two terms,

$$\tilde{\sigma}^{(3);dabc}(\omega, \omega_0, \omega_3) = \tilde{\sigma}_f^{(3);dabc}(\omega, \omega_0, \omega_3) + \tilde{\sigma}_t^{(3);dabc}(\omega, \omega_0, \omega_3),$$

where $\tilde{\sigma}_f^{(3);dabc}$ includes all terms in Eq. (9) in which v_3 appears, and $\tilde{\sigma}_t^{(3);dabc}$ includes all remaining terms. Note that $\tilde{\sigma}_f^{(3);dabc}$ is non-zero only for a doped system. Induced currents in this model flow in the plane in which the gapped graphene is assumed to lie, which we take to be the (xy) plane; $\sigma^{(3);dabc}$, $\tilde{\sigma}^{(3);dabc}$, and S_j^{dabc} are fourth rank tensors, each with 16 components, and the independent components can be taken to be those with the components $xyxy$, $xyxy$, and $xyyx$. The other nonzero components can be obtained through $S_j^{xxxx} = S_j^{xxyy} + S_j^{xyxy} + S_j^{xyyx}$, and the symmetry $\{x \leftrightarrow y\}$. We list the independent nonzero components of these tensors, taking $S_j^{dabc}(\dots)$ as an example, as a column vector

$$S_j = \begin{bmatrix} S_j^{xxyy} \\ S_j^{xyxy} \\ S_j^{xyyx} \end{bmatrix}.$$

For gapped graphene, the expressions for S_i show features similar to the corresponding expressions for graphene:⁴⁴ They are functions of the effective gap parameter $E_c = \max\{\Delta, |\mu|\}$ and Δ , in addition to the energies w , w_0 , and w_3 . In all these expressions, E_c appears only in functions of E_c^{-5} , E_c^{-3} , E_c^{-1} , $\mathcal{I}(E_c; w)$, $\mathcal{H}(E_c; w)$, $\mathcal{H}(E_c; w_0)$, $\mathcal{G}(E_c; w)$, $\mathcal{G}(E_c; w_0)$, and

$\mathcal{G}(E_c; w_3)$, where

$$\mathcal{G}(x; w) = \ln \left| \frac{w + 2x}{w - 2x} \right| + i \left(\pi + \arctan \frac{\text{Re}[w] - 2x}{\text{Im}[w]} - \arctan \frac{\text{Re}[w] + 2x}{\text{Im}[w]} \right), \quad (15)$$

$$\mathcal{H}(x; w) = \frac{1}{2x + w} + \frac{1}{2x - w}, \quad (16)$$

$$\mathcal{I}(x; w) = \frac{1}{(2x + w)^2} - \frac{1}{(2x - w)^2}. \quad (17)$$

We can write each S_j^{dabc} as a linear combination of these functions, with their arguments themselves being functions of w , w_0 , w_3 , and Δ . All terms can be expanded in even orders of Δ , particularly as functions proportional to Δ^0 , Δ^2 , and Δ^4 , as shown in Appendix B.

With all these analytic expressions in hand, any third order nonlinear conductivity can be calculated and studied directly. In the following, we consider the intraband divergences that are of interest here, by giving the leading contributions to the conductivities.

A. Current-Induced Second order Nonlinearity

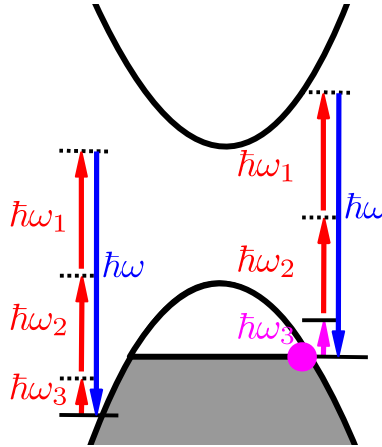


FIG. 1. Illustration of the excitation scenario for CISNL. A general transition process is sketched on the left hand side at a \mathbf{k} point away from the Fermi surface, and the intraband transition induced divergent term (as $\hbar\omega_3 \rightarrow 0$) is sketched on the right hand side; the latter occurs only for the electrons at the Fermi surface. The short dashed horizontal lines stand for virtual states.

We begin by considering the response coefficient $\sigma^{(3)dabc}(\omega_1, \omega_2, 0)$, where we assume that neither ω_1 nor ω_2 vanishes, and that their sum is finite. This describes a second-order optical nonlinearity induced by a DC field ($\omega_3 = 0$), and if there are free carriers we would expect a divergent contribution because of the large response of the free carriers to the DC field. A

picture of the excitation scenario is given in Fig. 1. In our expression for $\tilde{\sigma}^{(3);dabc}(\omega, \omega_0, \omega_3)$ the divergence of interest is clearly signaled by $v_3 \rightarrow 0$, and the divergent response term can be obtained from the analytic expressions. When this is isolated, the most important relaxation parameter is $\Gamma_a^{(1)}$, which we treat differently than we treat the other relaxation parameters; for $j = 2, 3$ we set $\Gamma_a^{(j)} = \Gamma_e^{(j)} = \Gamma$ to give $v = w$ and $v_0 = w_0$ in the expression for $\tilde{\sigma}^{(3);dabc}$. The divergent term can be written as

$$\tilde{\sigma}^{(3)}(\omega, \omega_0, \omega_3 \rightarrow 0) \approx \frac{i\sigma_3}{\Delta^5} \frac{E_c^2 - \Delta^2}{\hbar\omega_3 + i\Gamma_a^{(1)}} \mathcal{Z}_1 \left(\frac{w}{\Delta}, \frac{w_0}{\Delta}, \frac{E_c}{\Delta} \right), \quad (18)$$

with $\sigma_3 = \sigma_0(\hbar v_F e)^2/\pi$, $\sigma_0 = e^2/(4\hbar)$, and

$$\mathcal{Z}_1(x, x_0; \alpha) = \frac{-16}{\alpha x x_0 (x^2 - 4\alpha^2)^2 (x_0^2 - 4\alpha^2)} \left\{ \begin{array}{l} \left[\begin{array}{l} 4\alpha^2 x (2x + x_0) \\ -x^3 x_0 \\ x_0 (x^3 + x_0 (3x^2 - 4\alpha^2)) \end{array} \right] \\ + [4\alpha^2 (\alpha^2 + 3) - (3\alpha^2 + 1) x^2 - (x^2 + 4) x_0^2 - 2(\alpha^2 + 1) x_0 x] \begin{bmatrix} 1 \\ 1 \\ 1 \end{bmatrix} \end{array} \right\}. \quad (19)$$

These expressions have a number of interesting features: (1) The divergent term in Eq. (18) does not include any contributions from the \mathcal{G} functions, indicating immediately that it is the existence of free carriers that is important. Indeed, this can be immediately confirmed, for if the system is undoped we have $E_c = \Delta$, and the term in Eq. (18) vanishes. (2) The divergent term is inversely proportional to the relaxation parameter. Since in a very rough approximation the DC current satisfies $\mathbf{J}_{\text{DC}} \propto \left(\Gamma_a^{(1)}\right)^{-1} \mathbf{E}_{\text{DC}}$ with the DC field \mathbf{E}_{DC} , the divergent contribution to $\sigma^{(3);dabc}(\omega_1, \omega_2, 0)$ can be written as a finite term proportional to \mathbf{J}_{DC} , hence the identification of this response as “current-induced second order nonlinearity.” (3) The expression in Eq. (19) for $\mathcal{Z}_1(x, x_0; \alpha)$ can exhibit further divergences as $w \rightarrow 2E_c$ and $w_0 \rightarrow 2E_c$, indicating that interband divergences can arise in CISNL as well, depending on the values of the optical frequencies ω_1 and ω_2 .

We refer to the terms in $\sigma^{(3);dabc}(\omega_1, \omega_2, 0)$ that are *not* divergent as $v_3 \rightarrow 0$ as the “field-induced second order nonlinearity.” They exist in the absence of free carriers, and have an analogue in the field induced second order nonlinearity of usual semiconductors, which leads to processes such as electric-field induced second harmonic generation (EFISH).^{44,46} Adopting this perspective, we can write the effective second order conductivity $\sigma^{(2);dab}(\omega_1, \omega_2) =$

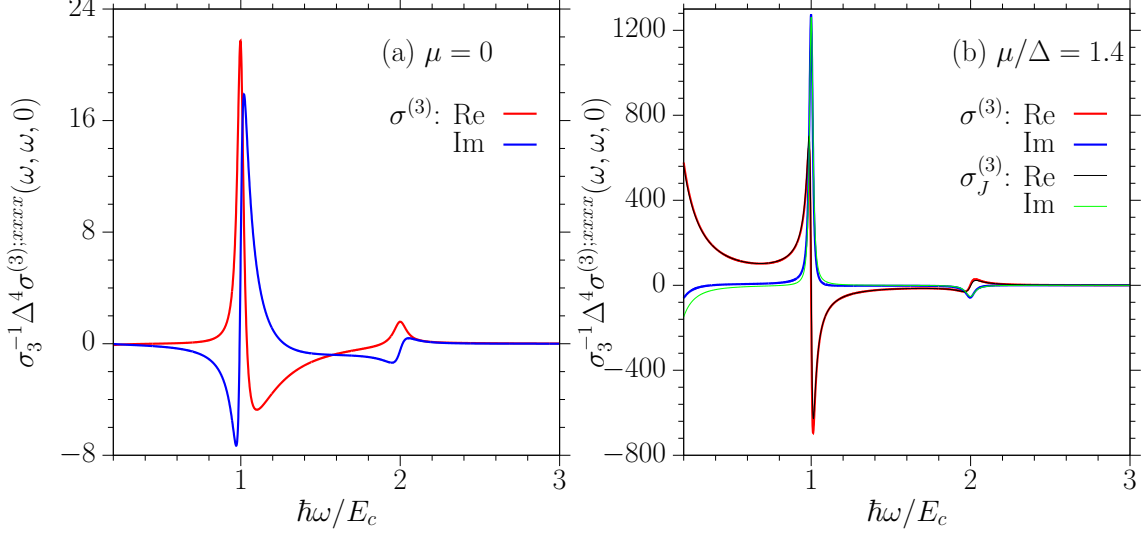


FIG. 2. Conductivity for second harmonic generation (a) $\mu = 0$ and (b) $\mu/\Delta = 1.4$ for $\Gamma/\Delta = 0.05$ and $\Gamma_a^{(3)}/\Delta = 0.01$. In (b), the current induced contribution is also plotted.

$3\sigma^{(3);dabc}(\omega_1, \omega_2, 0)E_{\text{DC}}^c$ with

$$\sigma^{(3);dabc}(\omega_1, \omega_2, 0) = \sigma_J^{(3);dabc}(\omega_1, \omega_2, 0) + \sigma_E^{(3);dabc}(\omega_1, \omega_2, 0). \quad (20)$$

The first term characterizes the current-induced second order response coefficient, and arises from the divergent contribution in Eq. (18),

$$\begin{aligned} \sigma_J^{(3);dabc}(\omega_1, \omega_2, 0) = \frac{\sigma_3 E_{\text{dc}}^c}{6\Gamma_a^{(1)}} \left[\left(\frac{E_c}{\Delta} \right)^2 - 1 \right] & \left[\mathcal{Z}_1^{dabc} \left(\frac{\hbar(\omega_1 + \omega_2) + i\Gamma}{\Delta}, \frac{\hbar\omega_2 + i\Gamma}{\Delta}; \frac{E_c}{\Delta} \right) \right. \\ & \left. + \mathcal{Z}_1^{dbac} \left(\frac{\hbar(\omega_1 + \omega_2) + i\Gamma}{\Delta}, \frac{\hbar\omega_1 + i\Gamma}{\Delta}; \frac{E_c}{\Delta} \right) \right]. \end{aligned} \quad (21)$$

All the remaining contributions are collected in the field induced response coefficient $\sigma_E^{(3);dabc}(\omega_1, \omega_2, 0)$.

Figure 2 shows the spectrum of $\sigma^{(3);xxxx}(\omega, \omega, 0)$ with a relaxation parameter $\Gamma/\Delta = 0.05$ for (a) an undoped system with no free carriers, $\mu/\Delta = 0$, and (b) a doped system with $\mu/\Delta = 1.4$. For both systems, there are obvious resonant peaks at $\hbar\omega = nE_c$ for $n = 1, 2$ associated with interband transitions; in the response of the doped system, there is an additional peak as $\hbar\omega \rightarrow 0$, and here the contribution from the current-induced SHG dominates for photon energies away from the resonances. This divergent process results in a qualitatively larger conductivity $\sigma^{(3);dabc}(\omega, \omega, 0)$ for a doped system (b) than for an undoped system (a).

B. Cross-Phase Modulation

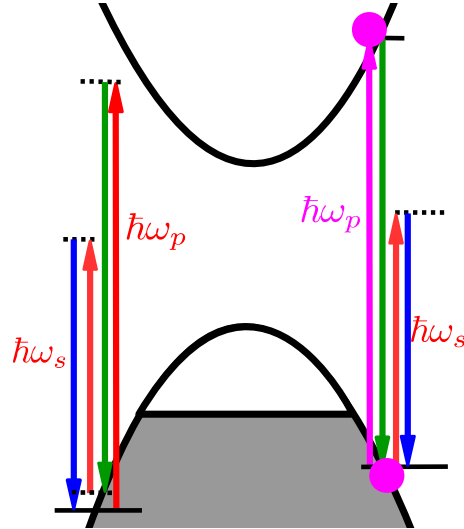


FIG. 3. Illustration of the excitation scenario for XPM. Similar to Fig. 1, the transition at the left hand side is off resonance, while the one at the right is on resonance.

In cross-phase modulation the propagation of light at frequency ω_s is modified by the presence of an intense optical field at a different frequency, ω_p ; it is characterized by the response coefficient $\sigma^{(3)}(\omega_s, -\omega_p, \omega_p)$. This conductivity exhibits a divergence as $w_0 \rightarrow 0$. Unlike CISNL, the divergence arises from the nonlinear response of the system and a static field is not required. The process is pictured in Fig. 3; we will see below that the divergent term vanishes unless $\hbar\omega_p$ is near or above the effective band gap $2E_c$. Cross-phase modulation of a signal frequency ω_s can be effected not just by a CW beam at ω_p , but by a pulse of light centered at such a frequency. So in general we seek $\sigma^{(3)}(\omega_s, -\omega_p + \delta, \omega_p)$, where knowledge of this expression for a small range of frequencies ω_p centered about a nominal pump frequency, and for a small range of detunings δ centered around zero, will allow us calculate the cross-phase modulation of a signal by a pump pulse. As $\delta, \Gamma_a^{(2)} \rightarrow 0$, the leading term of the relevant unsymmetrized conductivity is

$$\tilde{\sigma}^{(3)}(\omega_s + \delta, \delta \rightarrow 0, \omega_p) \approx \frac{i\sigma_3}{\Delta^3} \frac{2}{\hbar\delta + i\Gamma_a^{(2)}} \mathcal{Z}_2 \left(\frac{w}{\Delta}, \frac{w_3}{\Delta}, \frac{E_c}{\Delta} \right), \quad (22)$$

with $w = v = \hbar(\omega_s + \delta) + i\Gamma$, $w_3 = v_3 = \hbar\omega_p + i\Gamma$, where we set all first order and third

order relaxation energies to be the same for simplicity, and

$$\begin{aligned} \mathcal{Z}_2(x, x_3; \alpha) &= \frac{8(A_0 + 2xx_3A_4)}{x^3x_3^3\alpha} + \frac{8A_0}{3x^3x_3\alpha^3} + \frac{(x^2 - 4)^2A_0 + 4x^2(4 - x^2)A_5}{2x^4x_3}\mathcal{I}(\alpha; x) \\ &+ \frac{(x^2 - 4)^2A_0 + 32x^2A_5}{2x^5x_3}\mathcal{H}(\alpha; x) \\ &+ Z_1(x, x_3)\mathcal{G}(\alpha; x) + Z_2(x, x_3)\mathcal{G}(\alpha; x_3). \end{aligned} \quad (23)$$

and

$$Z_1(x, x_3) = \frac{x_3(x^2 - 4)^2A_0 + 32x^2(x_3A_5 + xA_4)}{2x^6(x^2 - x_3^2)}, \quad (24)$$

$$Z_2(x, x_3) = -\frac{x(x_3^2 - 4)^2A_0 + 32xx_3(x_3A_5 + xA_4)}{2x^2x_3^4(x^2 - x_3^2)}. \quad (25)$$

Here we used $A_0 = -(A_1 + A_2 + A_3)$, $A_4 = \frac{1}{4}(A_2 - A_3)$ and $A_5 = -\frac{1}{4}(2A_1 + A_2 + A_3)$, where

$$A_1 = \begin{bmatrix} -3 \\ 1 \\ 1 \end{bmatrix}, \quad A_2 = \begin{bmatrix} 1 \\ -3 \\ 1 \end{bmatrix}, \quad A_3 = \begin{bmatrix} 1 \\ 1 \\ -3 \end{bmatrix}. \quad (26)$$

We note that Z_1 and Z_2 themselves diverge as $x \rightarrow -x_3$ (i.e., $\omega_p \rightarrow \omega_s$), which will be discussed in next section.

Using the expression above we can write

$$\sigma^{(3)}(\omega_s, -\omega_p + \delta, \omega_p) = \sigma_{\text{xpm};d}^{(3)}(\omega_s, \omega_p; \delta) + \sigma_{\text{xpm}}^{(3)}(\omega_s, \omega_p; \delta), \quad (27)$$

where $\sigma_{\text{xpm};d}^{(3)}(\omega_s, \omega_p; \delta)$ contains a divergence with respect to $(\hbar\delta + i\Gamma_a^{(2)})^{-1}$

$$\begin{aligned} \sigma_{\text{xpm};d}^{(3);dabc}(\omega_s, \omega_p; \delta) &= \frac{i\sigma_3}{3\Delta^4} \left(\frac{\hbar\delta + i\Gamma_a^{(2)}}{\Delta} \right)^{-1} \left[\mathcal{Z}_2^{(3);dabc} \left(\frac{\hbar\omega_s + i\Gamma}{\Delta}, \frac{-\hbar\omega_p + i\Gamma}{\Delta}; \frac{E_c}{\Delta} \right) \right. \\ &\left. + \mathcal{Z}_2^{(3);dacb} \left(\frac{\hbar\omega_s + i\Gamma}{\Delta}, \frac{\hbar\omega_p + i\Gamma}{\Delta}; \frac{E_c}{\Delta} \right) \right], \end{aligned} \quad (28)$$

and $\sigma_{\text{xpm}}^{(3)}(\omega_s, \omega_p; \delta)$ contains the non-divergent response. Note that the divergent term is independent of the sequences of the limits $\delta \rightarrow 0$ and $\Gamma \rightarrow 0$.

Figure 4 gives the spectrum of $\sigma_{\text{xpm}}^{(3);xxxx}(\omega_s, \omega_p; 0)$, appropriate for CW illumination with the pump; as above we have taken a relaxation parameter $\Gamma/\Delta = 0.05$ and $\Gamma_a^{(2)}/\Delta = 0.01$, and again consider an undoped system ($\mu/\Delta = 0$) and a doped system with $\mu/\Delta = 1.4$. The complicated dependence of both the real and imaginary parts on the frequencies indicates the rich nature of the nonlinear response. The real parts show additional divergences as $\hbar\omega_s \rightarrow 0$

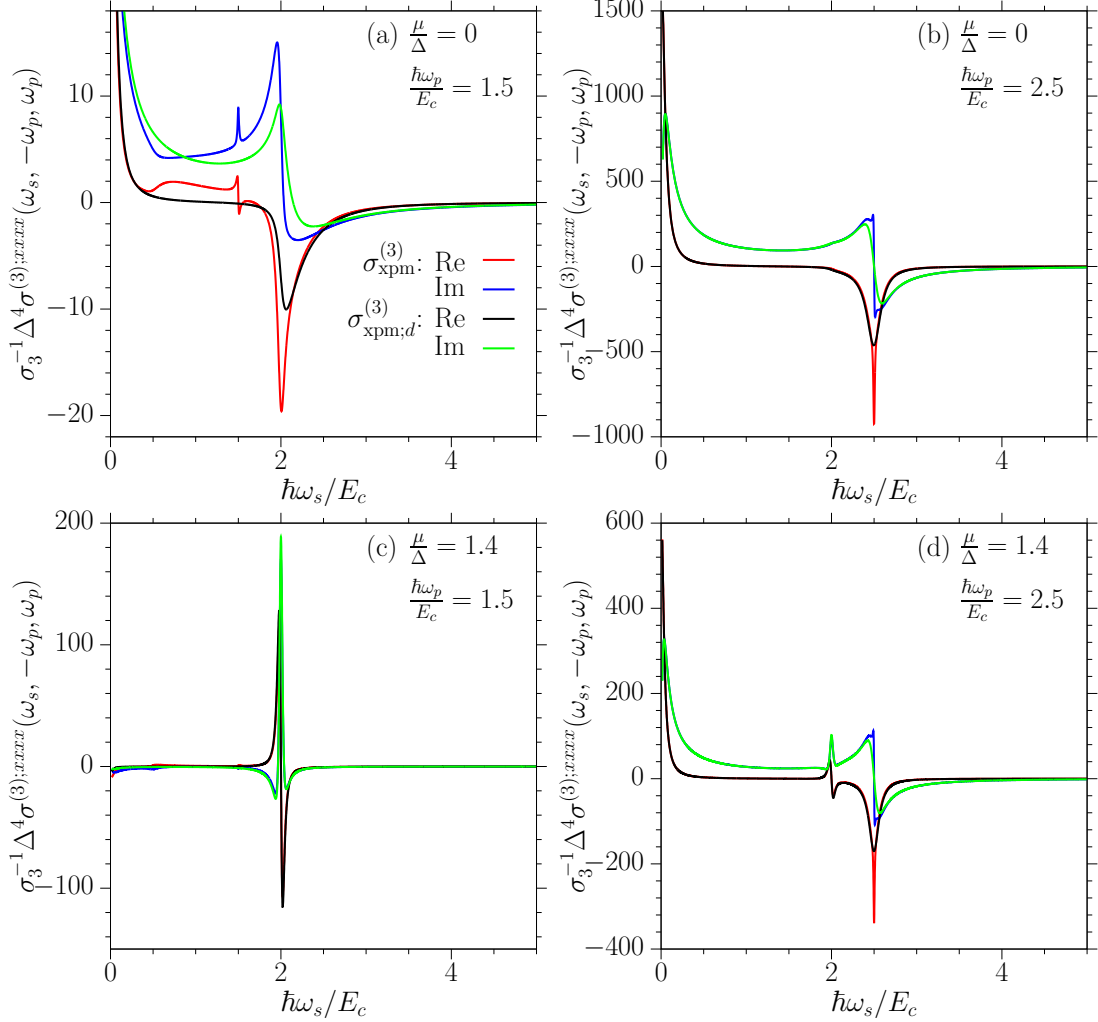


FIG. 4. Signal frequency ω_s dependence of the conductivity $\sigma_3^{-1}\Delta^4\sigma_{\text{xpm}}^{(3);xxxx}(\omega_s, \omega_p; 0)$ at different chemical potential and pump frequencies for $\Gamma/\Delta = 0.05$ and $\Gamma_a^{(2)}/\Delta = 0.01$. The parameters of $(\frac{\mu}{\Delta}, \frac{\hbar\omega_p}{E_c})$ are (a) (0, 1.5), (b) (0, 2.5), (c) (1.4, 1.5), and (d) (1.4, 2.5). The divergent contribution $\sigma_{\text{xpm};d}^{(3);xxxx}(\omega_s, \omega_p; 0)$ are also shown for comparison.

and $\hbar\omega_p \rightarrow 0$, as would be expected from the discussion of CISNL above, and as $\hbar\omega_s \rightarrow \hbar\omega_p$, as we discuss in the section below. As would be expected from the discussion of CISNL above, there are other divergences or resonant peaks associated with either $\hbar\omega_s \rightarrow 0$ or interband transitions; the latter are not our focus in this work. Away from these resonances, the values of the conductivity for the cases $\hbar\omega_p/E_c = 1.5$ are much smaller than those for the cases $\hbar\omega_p/E_c = 2.5$, which include the intraband divergences, and the contribution from $\sigma_{\text{xpm};d}^{(3);xxxx}(\omega_s, \omega_p; 0)$ is generally the largest part of $\sigma^{(3)}(\omega_s, -\omega_p, \omega_p)$ away from these other divergences. We can get some insight into the importance of pump frequency by noting that

as $\Gamma \rightarrow 0$ the divergent term $\sigma_{\text{xpm};d}^{(3);dabc}(\omega_s, \omega_p; \delta)$ becomes

$$\sigma_{\text{xpm};d}^{(3)}(\omega_s, \omega_p; \delta) \rightarrow \frac{i\sigma_3}{\Delta^4} \left(\frac{\hbar\delta + i\Gamma_a^{(2)}}{\Delta} \right)^{-1} h_1 \left(\frac{\hbar\omega_p}{\Delta}, \frac{\hbar\omega_s}{\Delta} \right) T \left(\frac{E_c}{\Delta}, \frac{\hbar\omega_p}{\Delta} \right) \quad (29)$$

with

$$h_1(x, x_1) = \frac{(x^2 - 4)^2 A_0 + 32x(xA_5 + x_1A_4)}{6x^4 x_1 (x^2 - x_1^2)} \quad (30)$$

and

$$T(y, x) = \mathcal{G}(y; x + i0^+) + \mathcal{G}(y; -x + i0^+) = 2i\pi\theta(x - 2y). \quad (31)$$

So in the clean limit, where all $\Gamma_{a/e}^{(j)} \rightarrow 0$, $\sigma_{\text{xpm};d}^{(3)}(\omega_s, \omega_p; \delta)$ vanishes if $\hbar\omega_p$ is below the effective gap $2E_c$. The frequency variation δ comes from the pumping beam, which is negligible for very long pulse duration; then $\sigma_{\text{xpm};d}^{(3)}$ is pure imaginary, and the modulation is associated with refraction rather than absorption. Deviations from this arise from the finite relaxation rate for other transition processes, but clearly this divergence is associated with resonant excitation from the valence to conduction band at $\hbar\omega_p$, as sketched in Fig. 3.

C. Degenerate Four Wave Mixing

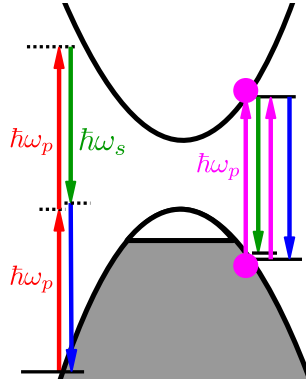


FIG. 5. Illustration of the excitation scenario for degeneration FWM. Similar to Fig. 1, the transition at the left hand side is off resonance, while the one at the right is on resonance.

In Eqs. (23) and (30) there appear to be divergences as $v \rightarrow \pm v_3$. Working out the expression in detail it can be immediately seen that in fact no divergence results as $v \rightarrow v_3$, but a divergence does indeed arise as $v \rightarrow -v_3$. The leading divergence is associated with

terms of the form $v_0^{-1}(v + v_3)^{-1}$. It gives a higher order divergence with a Lorentz type lineshape, as shown in Figs. 4 (b) and (d). Such a divergence also exists in the widely studied nonlinear phenomena of four-wave mixing, which is characterized by the response coefficient $\sigma^{(3)}(\omega_p, \omega_p, -\omega_s)$. As for XPM, the divergent point is at $\omega_s = \omega_p$, but since the generated field is at $2\omega_p - \omega_s$ rather than at ω_s the path to the divergence is different.

As $\omega_s \rightarrow \omega_p$, the divergent term arises in the unsymmetrized conductivities $\tilde{\sigma}^{(3)}(2\omega_p - \omega_s, \omega_p - \omega_s, -\omega_s)$ and $\tilde{\sigma}^{(3)}(2\omega_p - \omega_s, \omega_p - \omega_s, \omega_p)$. Taking $\delta = \omega_s - \omega_p$ and all $\Gamma_{a/e}^{(j)}$ as small quantities, the conductivity can be approximated as

$$\begin{aligned} \sigma^{(3)}(\omega_p, \omega_p, -\omega_s) \approx & \frac{i\sigma_3}{\Delta^4} \frac{\Delta}{\hbar\delta + i\Gamma_a^{(2)}} \left[\frac{\Delta}{\hbar\delta + i\Gamma} \mathcal{Z}_3 \left(\frac{\hbar\omega_p}{\Delta}, \frac{\Gamma}{\Delta}; \frac{E_c}{\Delta} \right) \right. \\ & \left. + \mathcal{Z}_4 \left(\frac{\hbar\omega_p}{\Delta}, \frac{\Gamma}{\Delta}; \frac{E_c}{\Delta} \right) \right]. \end{aligned} \quad (32)$$

Here we set all the relaxation parameters $\Gamma_{a/e}^{(j)}$ except $\Gamma_a^{(2)}$ equal to Γ . The exact expression can be obtained following Eq. (22), or even from the full expression in Appendix. B. The physics of this divergence can be revealed if we consider the clean limit for \mathcal{Z}_3 and \mathcal{Z}_4 . They are $\mathcal{Z}_j(x, 0; \alpha) = Z_j(x)T(\alpha, x)$ for $j = 3, 4$ with

$$Z_3(x) = \frac{1}{12x^6} [(x^4 + 24x^2 + 16)A_0 - 48x^2A_6] \quad (33)$$

$$Z_4(x) = \frac{1}{12x^7} [(x^4 - 56x^2 - 48)A_0 + 160x^2A_6], \quad (34)$$

with $A_6 = -(A_1 + A_2 + 2A_3)/4$. Here $T(\alpha; x)$ survives only for $x > 2\alpha$ (see Eq. (31)), where one photon absorption exists. Thus a relevant picture for this kind of resonance is shown in Fig. 5.

We illustrate these divergences in Fig. 6 for two different pump frequencies, $\hbar\omega_p/E_c = 1.5$ and 2.5. We plot the results for an undoped system, $|\mu|/\Delta = 0$, and a doped system with $|\mu|/\Delta = 1.4$. The conductivity strongly depends on the ratio $\hbar\omega/E_c$. For $\hbar\omega/(2E_c) < 1$, the divergent term vanishes in the clean limit and only the non-divergent term survives. The features in Fig. 6(a) as $\hbar\omega_s$ is around $\hbar\omega_p$ are induced by the nonzero relaxation parameters. For $\hbar\omega/(2E_c) > 1$ the divergent term survives and to leading order varies as $[\hbar\delta + i\Gamma_a^{(2)}]^{-1} (\hbar\delta + i\Gamma)^{-1}$, where we separate out the second order intraband relaxation parameter, and put the rest equal to Γ . The near degenerate FWM is approximately deter-

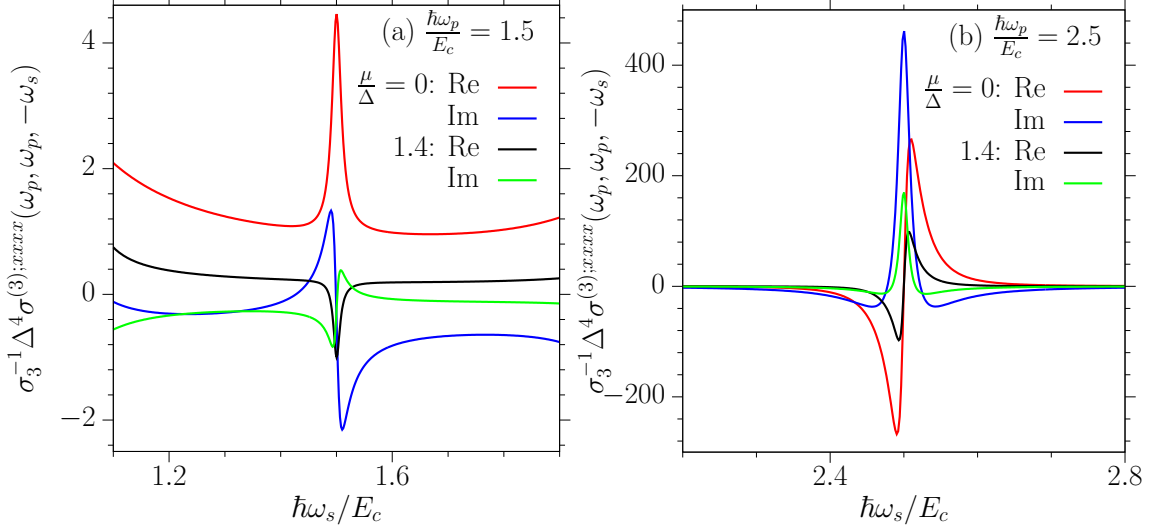


FIG. 6. Conductivity $\sigma^{(3);xxxx}(\omega_p, \omega_p, -\omega_s)$ for ω_s around ω_p at different chemical potential $|\mu|/\Delta = 0$ and 1.4 and different pump frequency $\hbar\omega_p/E_c = 1.5$ and 2.5. The relaxation parameters are taken as $\Gamma_a^{(2)}/\Delta = 0.01$ and $\Gamma/\Delta = 0.05$, and the gap parameter is taken as $\Delta = 1$ eV.

mined by

$$\sigma^{(3)}(\omega_p, \omega_p, -\omega_p + \delta) \approx -\frac{2\pi\sigma_3}{\Delta^2[\hbar\delta + i\Gamma_a^{(2)}](\hbar\delta + i\Gamma)} Z_3\left(\frac{\hbar\omega_p}{\Delta}\right) \times \theta(\hbar\omega_p - 2E_c).$$

Note that the nonlinear response to a pulse of light can be expected to be very complicated due to the strong dependence on the detuning.

D. Coherent Current Injection

Now we turn to another divergence associated with $v \rightarrow 0$ in Eq. (9), which exists in the conductivity $\sigma^{(3)}(-2\omega + \delta, \omega, \omega)$ as $\delta \rightarrow 0$. This divergence describes coherent current injection. Setting all the relaxation parameters $\Gamma_{a/e}^{(j)}$ except $\Gamma_a^{(3)}$ equal to Γ , we have the leading contribution with respect to the small quantity $\Gamma_a^{(3)}$ and δ given by

$$\sigma^{(3)}(-2\omega + \delta, \omega, \omega) = \frac{\eta_{cci}(\omega, \Gamma)}{\hbar^{-1}\Gamma_a^{(3)} - i\delta} + \dots \quad (35)$$

While the full expressions of $\eta_{cci}(\omega, \Gamma)$ can be obtained from our general analytic expressions, the underlying physics can be easily shown at the clean limit; setting $\Gamma \rightarrow 0^+$, we find

$$\eta_{cci}(\omega, 0) = \frac{\sigma_3}{\hbar\Delta^3} \left[g_1\left(\frac{\hbar\omega}{\Delta}\right) T\left(\frac{E_c}{\Delta}, \frac{2\hbar\omega}{\Delta}\right) + g_2\left(\frac{\hbar\omega}{\Delta}\right) T\left(\frac{E_c}{\Delta}, \frac{\hbar\omega}{\Delta}\right) \right], \quad (36)$$

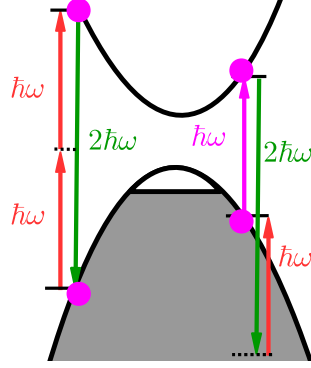


FIG. 7. Illustration of the excitation scenario for XPM. The transition at the left hand side corresponds to the interference between one-photon absorption and degenerate two-photon absorption, while the transition at the right hand side corresponds to the interference between one-photon absorption and the stimulated Raman process.

where the functions g_1 and g_2 are given by

$$g_1(x) = \frac{1}{3x^7} \left[(1-x^2)^2, 1-x^4, 1-x^4 \right]^T, \quad (37)$$

$$g_2(x) = \frac{1}{12x^7} \left[-16 + 24x^2 - 5x^4, -16 - 8x^2 + 3x^4, -16 - 8x^2 + 3x^4 \right]^T. \quad (38)$$

The coefficient η_{cci} describes the two-color coherent current injection coefficient. In the clean limit, it includes two terms: the one involving g_2 is nonzero only for $\hbar\omega > 2E_c$, and the one involving g_1 is nonzero for $\hbar\omega > E_c$. Both terms arise because of the interference of one-photon and two-photon absorption processes. However, the contribution from the term involving g_1 comes from the interference between the pathways of one-photon absorption and degenerate two-photon absorption, as illustrated in the transition process on the left side of Fig. 7. While the term involving g_2 comes from the interference between one-photon absorption and the stimulated Raman process, as shown in the transition process on the right side of Fig. 7. In experiments involving typical semiconductors $2\hbar\omega$ is usually greater than the band gap energy but $\hbar\omega$ is not; however, if $\hbar\omega$ also is greater than the gap there can be a contribution due to stimulated electronic Raman scattering. In the clean limit, a direct calculation of the functions $g_i(x)$ gives $g_1(1) = g_2(2) = 0$. For the component $\sigma^{(3);xxxx}$, their contributions are maximized at $x \approx 1.2$ for $g_1(x)$ and $x \approx 2.4$ for $g_2(x)$. However, at $x \approx 2.4$, the contribution from the stimulated electronic Raman scattering is no more than 20% of the contribution from the usual injection process; the total contribution has no maximum around $x \approx 2.4$.

A direct consequence of the divergence $v \rightarrow 0$ is the form of the current response to a pulse light. For simplicity, we only take the beam at 2ω as a pulse, and then the time evolution of the current density is

$$J^{(3);d}(t) = \int \frac{d\delta}{2\pi} \sigma^{(3);dabc}(-2\omega + \delta, \omega, \omega) E^a(-2\omega + \delta) E^b(\omega) E^c(\omega) e^{-i\delta t}. \quad (39)$$

With substitution of the leading term in Eq. (35) we can get

$$\frac{dJ^{(3);d}(t)}{dt} = \eta_{cci}^{dabc}(\omega, \Gamma) E_{2\omega}^a(t) E_{\omega}^b(t) E_{\omega}^c(t) - \hbar^{-1} \Gamma_a^{(3)} J^{(3);d}(t). \quad (40)$$

Here $\mathbf{E}_{2\omega}(t)$ and $\mathbf{E}_{\omega}(t)$ are the time evolution of pulses with center frequencies at 2ω and ω , respectively. The first term at the right hand side is a source term, while the second term describes the damping. This equation shows exactly how the injection process occurs.

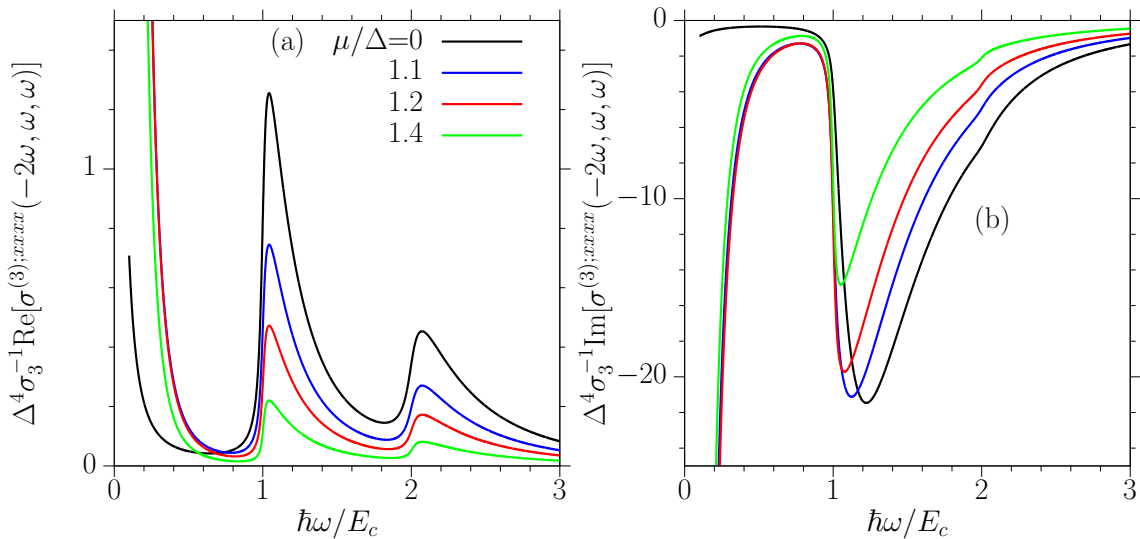


FIG. 8. Conductivity $\sigma^{(3);xxxx}(-2\omega, \omega, \omega)$ for different chemical potential $|\mu|/\Delta = 0, 1.1, 1.2,$ and 1.4 . The relaxation parameters are taken as $\Gamma_a^{(3)}/\Delta = 0.01$ and $\Gamma/\Delta = 0.05$, the gap parameter is taken as $\Delta = 1$ eV.

As an illustration, we plot the $\sigma^{(3);xxxx}(-2\omega, \omega, \omega)$ as a function of ω for different chemical potentials $|\mu|/\Delta = 0, 1.1, 1.2,$ and 1.4 ; the other parameters are taken as $\Gamma_a^{(3)}/\Delta = 0.01$, $\Gamma/\Delta = 0.05$, and $\Delta = 1$ eV. In the clean limit, $\sigma^{(3);xxxx}$ is purely imaginary, and although with the inclusion of damping the real parts do not vanish, they are about an order of magnitude smaller than the imaginary parts, as shown in Fig. 8. In the calculations at finite relaxation parameters, both the real and the imaginary parts show obvious peaks/valleys

around $\hbar\omega \sim E_c$ and $\hbar\omega \sim 2E_c$, which correspond to the contributions from the terms including g_1 and g_2 , respectively. In contrast to the situation discussed after Eq. (38) for clean limits, the appearance of the peaks for $\hbar\omega > 2E_c$ arises because of the inclusion of the finite relaxation parameters. There also exists increases of the conductivity values as $\hbar\omega \rightarrow 0$, mostly for nonzero μ/Δ . They are associated with a divergence induced by the free-carriers, which is not our focus in this work.

E. Jerk Current

Some of the divergences considered here can appear simultaneously. A good example is the recently discussed jerk current,³² which can be treated as a special case of XPM for a zero signal frequency, or a special case of CISNL for current induced one-photon current injection. The corresponding conductivity is $\sigma^{(3);dabc}(\omega, -\omega, 0)$, which involves the unsymmetrized conductivities $\tilde{\sigma}^{(3);dabc}(0, -\omega, 0)$, $\tilde{\sigma}^{(3);dacb}(0, -\omega, -\omega)$, $\tilde{\sigma}^{(3);dbac}(0, \omega, 0)$, $\tilde{\sigma}^{(3);dbca}(0, \omega, \omega)$, $\tilde{\sigma}^{(3);dcab}(0, 0, -\omega)$, and $\tilde{\sigma}^{(3);dcba}(0, \omega, 0)$. They all include intraband divergences, and the highest order is described by the limiting behavior as $v, v_0 \rightarrow 0$ or $v, v_3 \rightarrow 0$. In general, the leading orders are

$$\sigma^{(3);dabc}(\omega, -\omega, 0) \approx \frac{i\sigma_3}{\Delta^4} \frac{\Delta}{i\Gamma_a^{(3)}} \left[\frac{\Delta}{i\Gamma_a^{(2)}} Q_1 \left(\frac{\hbar\omega}{\Delta}; \left\{ \frac{\Gamma_{a/e}^{(j)}}{\Delta} \right\} \right) + \frac{\Delta}{i\Gamma_a^{(1)}} Q_2 \left(\frac{\hbar\omega}{\Delta}; \left\{ \frac{\Gamma_{a/e}^{(j)}}{\Delta} \right\} \right) \right]. \quad (41)$$

The clean limits of Q_1 and Q_2 are

$$Q_1(x; 0) = \frac{1}{6x^6} [(x^2 - 4)^2 A_0 + 32x^2 A_6] T(\alpha; x), \quad (42)$$

$$Q_2(x; 0) = \frac{(\alpha^2 - 1)(\alpha^2 + 3)}{3\alpha^5} \frac{1}{x} A_0, \quad (43)$$

with $\alpha = E_c/\Delta$. Here $Q_1(x; 0)$ is nonzero only when the one-photon absorption exists as $\hbar\omega > 2E_c$, while $Q_2(x; 0)$ exists only for a doped system where $\alpha > 1$. These two terms have a different power dependence, and the term involving $Q_2(x; 0)$ can exist for any optical field frequency. Thus the frequency dependence of the response can be used to distinguish between them.

IV. COMPARISON WITH GRAPHENE

Some of the phenomena discussed above have been considered earlier for doped graphene.^{19,44,47} Although the expressions we derived above are normalized to the gap parameter Δ , it is

safe to take the limit as $\Delta \rightarrow 0$. This is because our general expressions of the conductivity can be safely reduced to the case of graphene with taking $\Delta = 0$, as shown in Appendix B. The results of CISNL, DFWM, and CCI in graphene have been discussed earlier^{19,44,47} in the clean limit and with finite relaxation parameters. Here we give a brief discussion for XPM and the jerk current in graphene. In the clean limit, the XPM for graphene can be found from Eq. (29) to be

$$\sigma_{\text{xpm};d}^{(3)}(\omega_s, \omega_p; \delta) \rightarrow \frac{i\sigma_3}{\hbar\delta} \frac{T(|\mu|; \hbar\omega_p)}{12\hbar\omega_s[(\hbar\omega_p)^2 - (\hbar\omega_s)^2]} A_0, \quad (44)$$

Here the chemical potential induced gap plays a role similar to that of the gap parameter in gapped graphene. For the jerk current, the leading term becomes

$$\sigma^{(3);dabc}(\omega, -\omega, 0) \rightarrow \frac{\sigma_3}{3i\Gamma_a^{(3)}} \left[\frac{1}{\Gamma_a^{(2)}} \frac{T(|\mu|; \hbar\omega)}{2(\hbar\omega)^2} + \frac{1}{\Gamma_a^{(1)}} \frac{1}{|\mu|(\hbar\omega)} \right] A_0. \quad (45)$$

V. CONCLUSIONS

We have systematically discussed intraband divergences in the third order optical response, and identified the leading terms in the corresponding third order conductivity. Due to the combination of intraband and interband transitions, these divergences can appear at optical frequencies, and lead to large nonlinear conductivities. We have shown that the existence of such divergences is very general, independent of the details of the band structure. We illustrated these divergences in gapped graphene, with analytic expressions obtained for the third order conductivities in the relaxation time approximation.

Such divergences are of interest to experimentalists, because within the independent particle treatment presented here the optical response is limited only by the phenomenological relaxation times introduced in the theory, and thus that optical response can be expected to be large. As well, at a qualitative level the predicted nature of the divergent behavior is robust against approximations made in describing the details of the interband transitions. The divergences are also of interest to theorists, because one can expect that under such conditions the kind of treatment presented here is too naive. This could be both because more realistic treatments of relaxation processes are required, and as well because the large optical response predicted could be an indication that in a real experimental scenario the perturbative approach itself is insufficient. Thus the identification of these divergences identifies regions of parameter space where experimental and theoretical studies can be expected

to lead to new insights into the nature of the interaction of light with matter.

More generally, we can expect that the calculation of other response coefficients involving perturbative expressions of the density matrix response to an electric field will reveal similar divergences in the nonlinear contributions to the response of other physical quantities, such as carrier density, spin/valley polarization, and spin/valley current. A deep understanding of these divergences can lead to new ways to probe these quantities, and to study new effects in the optical response of materials that depend on them.

ACKNOWLEDGMENTS

This work has been supported by CAS QYZDB-SSW-SYS038, NSFC Grant No. 11774340 and 61705227. S.W.W. is supported by the National Basic Research Program of China under Grant No. 2014CB921601S. J.E.S. is supported by the Natural Sciences and Engineering Research Council of Canada.

Appendix A: Perturbative conductivity for general band structure

In this appendix we give the formal derivation of the third order conductivities in terms of the electron energy, velocity matrix elements, and Berry connections. The density matrix can be expanded in terms of electric fields as

$$\begin{aligned} \rho_{nm\mathbf{k}}(t) &= \sum_{\omega_3} \tilde{\mathcal{P}}_{nm\mathbf{k}}^{(1);c}(\omega_3) E^c(\omega_3) e^{-i\omega_3 t} \\ &+ \sum_{\omega_2 \omega_3} \tilde{\mathcal{P}}_{nm\mathbf{k}}^{(2);bc}(\omega_0, \omega_3) E^b(\omega_2) E^c(\omega_3) e^{-i\omega_0 t} \\ &+ \sum_{\omega_1 \omega_2 \omega_3} \tilde{\mathcal{P}}_{nm\mathbf{k}}^{(3);abc}(\omega, \omega_0, \omega_3) E^a(\omega_1) E^b(\omega_2) E^c(\omega_3) e^{-i\omega t} + \dots, \end{aligned} \quad (\text{A1})$$

with $\omega = \omega_1 + \omega_2 + \omega_3$ and $\omega_0 = \omega_2 + \omega_3$. Using the iteration in Eq. (5), we can get the density matrix at different perturbation orders. The first order terms of the density matrix are

$$\tilde{\mathcal{P}}_{nm\mathbf{k}}^{(1);c}(\omega_3) = \frac{1}{v_3} A_{1;nm\mathbf{k}}^{(1);c}, \quad A_{1;nm\mathbf{k}}^{(1);c} = i \frac{\partial f_{n\mathbf{k}}}{\partial k_a}, \quad (\text{A2})$$

$$\tilde{\mathcal{P}}_{nm\mathbf{k}}^{(1);c}(\omega_3) = B_{1;nm\mathbf{k}}^{(1);c}(\omega_3), \quad B_{1;nm\mathbf{k}}^{(1);c}(\omega_3) = \frac{r_{nm\mathbf{k}}^a f_{m\mathbf{k}}}{\omega_3 - (\varepsilon_{n\mathbf{k}} - \varepsilon_{m\mathbf{k}})}. \quad (\text{A3})$$

The second order terms are

$$\tilde{\mathcal{P}}_{n\mathbf{n}\mathbf{k}}^{(2);bc}(\omega_2, \omega_3) = \frac{1}{v_0 v_3} A_{1;n\mathbf{n}\mathbf{k}}^{(2);bc} + \frac{1}{v_0} A_{2;n\mathbf{n}\mathbf{k}}^{(3);bc}(w_3), \quad (\text{A4})$$

$$\tilde{\mathcal{P}}_{n\mathbf{m}\mathbf{k}}^{(2);bc}(\omega_2, \omega_3) = \frac{1}{v_3} B_{1;n\mathbf{m}\mathbf{k}}^{(2);bc}(w_0) + B_{2;n\mathbf{m}\mathbf{k}}^{(2);bc}(w_0, w_3), \quad (\text{A5})$$

with

$$A_{1;n\mathbf{n}\mathbf{k}}^{(2);bc} = i \frac{\partial A_{1;n\mathbf{n}\mathbf{k}}^{(1);c}}{\partial k_b}, \quad (\text{A6})$$

$$A_{2;n\mathbf{n}\mathbf{k}}^{(2);bc}(w_3) = \sum_m [r_{n\mathbf{m}\mathbf{k}}^b B_{1;m\mathbf{n}\mathbf{k}}^{(1);c}(w_3) - B_{1;n\mathbf{m}\mathbf{k}}^{(1);c}(w_3) r_{m\mathbf{n}\mathbf{k}}^b], \quad (\text{A7})$$

$$B_{1;n\mathbf{m}\mathbf{k}}^{(2);bc}(w_0) = \frac{r_{n\mathbf{m}\mathbf{k}}^b [A_{1;m\mathbf{m}\mathbf{k}}^{(1);c} - A_{1;n\mathbf{n}\mathbf{k}}^{(1);c}]}{w_0 - (\varepsilon_{n\mathbf{k}} - \varepsilon_{m\mathbf{k}})}, \quad (\text{A8})$$

$$B_{2;n\mathbf{m}\mathbf{k}}^{(2);bc}(w_0, w_3) = \frac{[r_{\mathbf{k}}^b, B_{1;\mathbf{k}}^{(1);c}(w_3)]_{nm} + i \left(B_{1;\mathbf{k}}^{(1);c}(w_3) \right)_{;nmk_b}}{w_0 - (\varepsilon_{n\mathbf{k}} - \varepsilon_{m\mathbf{k}})}. \quad (\text{A9})$$

Here we have used the notation $\mathbf{r}_{n\mathbf{m}\mathbf{k}} = (1 - \delta_{nm}) \boldsymbol{\xi}_{n\mathbf{m}\mathbf{k}}$ and

$$\left(B_{1;\mathbf{k}}^{(1);c}(w_3) \right)_{;nmk_b} = \frac{\partial B_{1;n\mathbf{m}\mathbf{k}}^{(1);c}(w_3)}{\partial k_b} - i(\xi_{n\mathbf{n}\mathbf{k}}^b - \xi_{m\mathbf{m}\mathbf{k}}^b) B_{1;n\mathbf{m}\mathbf{k}}^{(1);c}(w_3). \quad (\text{A10})$$

It shows that the diagonal terms of the Berry connections $\boldsymbol{\xi}_{n\mathbf{n}\mathbf{k}}$ appear always with the derivative $\nabla_{\mathbf{k}}$ to form a gauge invariant term.¹¹ The third order terms are

$$\begin{aligned} \tilde{\mathcal{P}}_{n\mathbf{n}\mathbf{k}}^{(3);abc}(\omega_1, \omega_2, \omega_3) &= \frac{1}{v v_0 v_3} A_{1;n\mathbf{n}\mathbf{k}}^{(3);abc} + \frac{1}{v v_0} A_{2;n\mathbf{n}\mathbf{k}}^{(3);abc}(w_3) \\ &+ \frac{1}{v v_3} A_{3;n\mathbf{n}\mathbf{k}}^{(3);abc}(w_0) + \frac{1}{v} A_{4;n\mathbf{n}\mathbf{k}}^{(3);abc}(w_0, w_3), \end{aligned} \quad (\text{A11})$$

$$\begin{aligned} \tilde{\mathcal{P}}_{n\mathbf{m}\mathbf{k}}^{(3);abc}(\omega_1, \omega_2, \omega_3) &= \frac{1}{v_0 v_3} B_{1;n\mathbf{m}\mathbf{k}}^{(3);abc}(w) + \frac{1}{v_0} B_{2;n\mathbf{m}\mathbf{k}}^{(3);abc}(w, w_3) \\ &+ \frac{1}{v_3} B_{3;n\mathbf{m}\mathbf{k}}^{(3);abc}(w, w_0) + B_{4;n\mathbf{m}\mathbf{k}}^{(3);abc}(w, w_0, w_3), \end{aligned} \quad (\text{A12})$$

with

$$A_{1;n\mathbf{n}\mathbf{k}}^{(3);abc} = i \frac{\partial A_{1;n\mathbf{n}\mathbf{k}}^{(2);bc}}{\partial k_a}, \quad (\text{A13})$$

$$A_{2;n\mathbf{n}\mathbf{k}}^{(3);abc}(w_3) = i \frac{\partial A_{2;n\mathbf{n}\mathbf{k}}^{(2);bc}(w_3)}{\partial k_a}, \quad (\text{A14})$$

$$A_{3;n\mathbf{n}\mathbf{k}}^{(3);abc}(w_0) = \sum_m [r_{n\mathbf{m}\mathbf{k}}^a B_{1;m\mathbf{n}\mathbf{k}}^{(2);bc}(w_0) - B_{1;n\mathbf{m}\mathbf{k}}^{(2);bc}(w_0) r_{m\mathbf{n}\mathbf{k}}^a], \quad (\text{A15})$$

$$A_{4;n\mathbf{n}\mathbf{k}}^{(3);abc}(w_0, w_3) = \sum_m [r_{n\mathbf{m}\mathbf{k}}^a B_{2;m\mathbf{n}\mathbf{k}}^{(2);bc}(w_0, w_3) - B_{2;n\mathbf{m}\mathbf{k}}^{(2);bc}(w_0, w_3) r_{m\mathbf{n}\mathbf{k}}^a], \quad (\text{A16})$$

and

$$B_{1;n\mathbf{k}}^{(3);abc}(w) = \frac{r_{n\mathbf{k}}^b [A_{1;m\mathbf{k}}^{(2);bc} - A_{1;n\mathbf{k}}^{(2);bc}]}{w - (\varepsilon_{n\mathbf{k}} - \varepsilon_{m\mathbf{k}})}, \quad (\text{A17})$$

$$B_{2;n\mathbf{k}}^{(3);abc}(w, w_3) = \frac{r_{n\mathbf{k}}^b [A_{2;m\mathbf{k}}^{(2);bc}(w_3) - A_{2;n\mathbf{k}}^{(2);bc}(w_3)]}{w - (\varepsilon_{n\mathbf{k}} - \varepsilon_{m\mathbf{k}})}, \quad (\text{A18})$$

$$B_{3;n\mathbf{k}}^{(3);abc}(w, w_0) = \frac{[r_{\mathbf{k}}^a, B_{1;\mathbf{k}}^{(2);bc}(w_0)]_{nm} + i \left(B_{1;\mathbf{k}}^{(2);bc}(w_0) \right)_{;nm\mathbf{k}_a}}{w - (\varepsilon_{n\mathbf{k}} - \varepsilon_{m\mathbf{k}})}, \quad (\text{A19})$$

$$B_{4;n\mathbf{k}}^{(3);abc}(w, w_0, w_3) = \frac{[r_{\mathbf{k}}^a, B_{2;\mathbf{k}}^{(2);bc}(w_0, w_3)]_{nm} + i \left(B_{2;\mathbf{k}}^{(2);bc}(w_0) \right)_{;nm\mathbf{k}_a}}{w - (\varepsilon_{n\mathbf{k}} - \varepsilon_{m\mathbf{k}})} \quad (\text{A20})$$

The current density is then calculated through $\mathbf{J}(t) = e \sum_{nm} \int \frac{d\mathbf{k}}{(2\pi)^2} v_{m\mathbf{k}}^d \rho_{nm\mathbf{k}}(t)$, and the S_j terms are given by

$$S_i^{dabc}(\dots) = -e^4 \sum_n \int \frac{d\mathbf{k}}{(2\pi)^2} v_{n\mathbf{k}}^a A_{i;n\mathbf{k}}^{(3);abc}(\dots), \quad \text{for } i = 1, 2, 3, 4, \quad (\text{A21})$$

$$S_i^{dabc}(\dots) = -e^4 \sum_{nm} \int \frac{d\mathbf{k}}{(2\pi)^2} v_{m\mathbf{k}}^a B_{i;n\mathbf{k}}^{(3);abc}(\dots), \quad \text{for } i = 5, 6, 7, 8. \quad (\text{A22})$$

Appendix B: S_j^{dabc} for a gapped graphene

The calculation of S_j^{dabc} is straightforward. In the linear dispersion approximation and relaxation time approximation, analytic expressions can be obtained. By listing the nonzero

components of $S_j^{dabc}(\dots)$ as a column vector $S_j = \begin{bmatrix} S_j^{xxyy} \\ S_j^{xyxy} \\ S_j^{xyyx} \end{bmatrix}$, we can write

$$\begin{aligned} S_j &= i\sigma_3 \left[W_j^{(0)} + 2\Delta^2 W_j^{(2)} + 2\Delta^4 W_j^{(4)} \right] \theta(|\mu| - \Delta), & \text{for } j = 1, 3, 5, 7, \\ S_j &= i\sigma_3 \left[W_j^{(0)} + 2\Delta^2 W_j^{(2)} + 2\Delta^4 W_j^{(4)} \right], & \text{for } j = 2, 4, 6, 8. \end{aligned} \quad (\text{B1})$$

with

$$\sigma_3 = \sigma_0 \frac{(\hbar v_F e)^2}{\pi}, \quad \sigma_0 = \frac{e^2}{4\hbar}. \quad (\text{B2})$$

Note that $W^{(j)}(\dots)$ depends on these functions

$$\begin{aligned} &|E_c|^{-5}, \quad |E_c|^{-3}, \quad |E_c|^{-1}, \\ &\mathcal{I}(E_c; w), \quad \mathcal{H}(E_c; w), \quad \mathcal{H}(E_c; w_0), \\ &\mathcal{G}(E_c; w), \quad \mathcal{G}(E_c; w_0), \quad \mathcal{G}(E_c; w_3). \end{aligned}$$

These functions depend on the photon energies and the effective gap parameter E_c .

1. $W_j^{(0)}$

Gapped graphene reduces to graphene⁴⁴ as $\Delta \rightarrow 0$ and $E_c \rightarrow |\mu|$, and thus $W_j^{(0)}$ should give the results for graphene, as

$$W_1^{(0)} = \frac{1}{E_c} A_0, \quad (\text{B3a})$$

$$W_3^{(0)}(w_0) = \mathcal{H}(E_c; w_0) \frac{A_3}{w_0} - \frac{1}{E_c} \frac{A_3}{w_0}, \quad (\text{B3b})$$

$$W_5^{(0)}(w) = \mathcal{H}(E_c; w) \frac{A_0}{w} + \mathcal{I}(E_c; w) A_1 - \frac{1}{E_c} \frac{A_0}{w}, \quad (\text{B3c})$$

$$W_7^{(0)}(w, w_0) = \mathcal{H}(E_c; w_0) \left(\frac{A_2}{w_1^2} - \frac{A_3}{w_0 w_1} \right) + \mathcal{H}(E_c; w) \left(\frac{A_3}{w w_1} - \frac{A_2}{w_1^2} \right) - \mathcal{I}(E_c; w) \frac{A_2}{w_1} + \frac{1}{E_c} \frac{A_3}{w w_0}, \quad (\text{B3d})$$

$$W_2^{(0)}(w_3) = \mathcal{G}(E_c; w_3) \frac{A_0}{w_3^2} - \frac{1}{E_c} \frac{A_0}{w_3}, \quad (\text{B3e})$$

$$W_4^{(0)}(w_0, w_3) = -\mathcal{G}(E_c; w_3) \frac{w_3 A_2 + w_2 A_3}{w_2^2 w_3^2} + \mathcal{G}(E_c; w_0) \frac{(w_0 + w_2) A_2 + w_2 A_3}{w_0^2 w_2^2} - \mathcal{H}(E_c; w_0) \frac{A_2}{w_0 w_2} + \frac{1}{E_c} \frac{A_3}{w_0 w_3}, \quad (\text{B3f})$$

$$W_6^{(0)}(w, w_3) = -\mathcal{G}(E_c; w_3) \frac{w A_0}{w_3^2 (w^2 - w_3^2)} + \mathcal{G}(E_c; w) \frac{w_3 A_0}{w^2 (w^2 - w_3^2)} + \frac{1}{E_c} \frac{A_0}{w w_3}, \quad (\text{B3g})$$

and

$$\begin{aligned} & W_8^{(0)}(w, w_0, w_3) \\ &= \mathcal{G}(E_c; w_3) \left[\frac{A_2}{(w - w_3) w_2^2 w_3} + \frac{w^2 w_2 + w_3^3 + w w_3 (-3w_0 + 2w_3)}{(w - w_3)^3 w_2^2 w_3^2} A_3 \right] \\ &+ \mathcal{G}(E_c; w_0) \left[-\frac{w_0 w_1 + w_1 w_2 - w_0 w_2}{w_0^2 w_1^2 w_2^2} A_2 - \frac{w_1 w_2 - w_0^2 - w_0 w_2}{w_1^2 w_0^2 w_2^2} A_3 \right] \\ &+ \mathcal{G}(E_c; w) \left[-\frac{1}{w w_1^2 (w - w_3)} A_2 - \frac{5w^2 + w_3 (w_0 + w_3) - w (3w_0 + 4w_3)}{w w_1^2 (w - w_3)^3} A_3 \right] \\ &+ \mathcal{H}(E_c; w_0) \left(\frac{A_2}{w_0 w_1 w_2} - \frac{A_3}{w_1^2 w_2} \right) + \mathcal{H}(E_c; w) \frac{4w^2 - 3w w_0 - 2w w_3 + w_0 w_3}{w w_1^2 (w - w_3)^2} A_3 \\ &+ \mathcal{I}(E_c; w) \frac{A_3}{w_1 (w - w_3)} - \frac{1}{E_c} \frac{A_3}{w w_0 w_3}. \end{aligned} \quad (\text{B3h})$$

Here we have used $w_2 = w_0 - w_3$, $w_1 = w - w_0$, and A_i defined in Eq. (26).

2. $W_j^{(2)}$

The Δ^2 terms are given as

$$W_1^{(2)} = \frac{1}{E_c^3} A_0, \quad (\text{B4a})$$

$$W_3^{(2)}(w_0) = \left[-\frac{1}{E_c^3} \frac{1}{2w_0} - \frac{1}{E_c} \frac{2}{w_0^3} + \mathcal{H}_{E_c}(w_0) \frac{2}{w_0^3} \right] (A_1 + A_2), \quad (\text{B4b})$$

$$W_5^{(2)}(w) = -\frac{1}{E_c^3} \frac{A_0}{w} - \mathcal{I}(E_c; w) \frac{2A_0 + 2A_1}{w^2} + \frac{1}{E_c} \frac{4A_1}{w^3} - \mathcal{H}(E_c; w) \frac{4A_1}{w^3}, \quad (\text{B4c})$$

$$\begin{aligned} W_7^{(2)}(w, w_0) &= \frac{1}{E_c^3} \frac{A_1 + A_2}{2ww_0} + \frac{1}{E_c} \left[\frac{2(w^2 - w_0^2)(A_1 + A_3)}{w^3 w_0^3} + \frac{2(w^3 - w_0^3)(A_2 - A_3)}{w_1 w^3 w_0^3} \right] \\ &\quad - \mathcal{I}(E_c; w) \frac{2(A_1 + A_3)}{w^2 w_1} + \mathcal{H}(E_c; w) \frac{(-4w + 2w_0)(A_1 + A_3) + 2w_1(A_2 - A_3)}{w^3 w_1^2} \\ &\quad + \mathcal{H}(E_c; w_0) \frac{-2w_1(A_1 + A_2) + 2w_0(A_1 + A_3)}{w_1^2 w_0^3}, \end{aligned} \quad (\text{B4d})$$

and

$$W_2^{(2)}(w_3) = \left\{ \frac{1}{E_c^3} \frac{1}{3w_3} + \frac{1}{E_c} \frac{4}{w_3^3} - \mathcal{G}(E_c; w_3) \frac{4}{w_3^3} \right\} A_1, \quad (\text{B4e})$$

$$\begin{aligned} W_4^{(2)}(w_0, w_3) &= \frac{1}{E_c^3} \frac{-A_1 + A_2 - 2A_3}{6w_0 w_3} \\ &\quad + \frac{1}{E_c} \left[-\frac{2(w_0^2 - w_3^2)(A_1 + A_3)}{w_0^3 w_3^3} + \frac{2(w_0^3 - w_3^3)(A_2 - A_3)}{w_2 w_0^3 w_3^3} \right] \\ &\quad - \mathcal{H}(E_c; w_0) \frac{A_1 + A_3}{w_0 w_2} \\ &\quad + \mathcal{G}(E_c; w_0) \frac{2w_0(A_1 + A_3) + 2w_2(A_1 - A_0)}{w_0^4 w_2^2} \\ &\quad + \mathcal{G}(E_c; w_3) \frac{(2w_0 - 4w_3)(A_1 + A_3) - 2w_2(A_2 - A_3)}{w_2^2 w_3^4}, \end{aligned} \quad (\text{B4f})$$

$$\begin{aligned} W_6^{(2)}(w, w_3) &= -\frac{1}{E_c^3} \frac{A_1}{3ww_3} + \frac{1}{E_c} \left[-\frac{4(w^2 + w_3^2)A_1}{w^3 w_3^3} + \frac{4(A_2 - A_3)}{w^2 w_3^2} \right] \\ &\quad + \mathcal{G}(E_c; w) \frac{-4w_3 A_1 + 4w(A_2 - A_3)}{w^4 (w^2 - w_3^2)} \\ &\quad + \mathcal{G}(E_c; w_3) \frac{4w A_1 - 4w_3(A_2 - A_3)}{w_3^4 (w^2 - w_3^2)}, \end{aligned} \quad (\text{B4g})$$

and

$$\begin{aligned}
& W_8^{(2)}(w, w_0, w_3) \\
= & \frac{1}{E_c^3} \frac{A_1 - A_2 + 2A_3}{6ww_0w_3} + \frac{1}{E_c} \left\{ \frac{2[w_0^2w_3^2 + w^2(w_0^2 - w_3^2)](A_1 - A_2 + 2A_3)}{w^3w_0^3w_3^3} \right. \\
& \left. + \frac{2[w_0(2w_0 + w_3) + w(w_0 + 2w_3)](-A_2 + A_3)}{w^2w_0^3w_3^2} \right\} \\
& + \mathcal{I}(E_c; w) \frac{2(A_1 + A_2)}{w^2w_1(w - w_3)} \\
& + \mathcal{H}(E_c; w) \frac{2(6ww_1 + ww_2 - 3w_1w_3)(A_1 + A_2)}{w^3w_1^2(w - w_3)^2} \\
& - \mathcal{G}(E_c; w) \left[\frac{2(6ww_1 + ww_2 - 3w_1w_3)(A_1 + A_2)}{w^3w_1^2(w - w_3)^3} - \frac{2(3w - 2w_0)}{w^4w_1^2(w - w_3)}(A_0 - A_1) \right] \\
& - \mathcal{H}(E_c; w_0) \frac{2w_1(A_1 + A_3) - 2w_0(A_1 + A_2)}{w_1^2w_0^3w_2} \\
& + \mathcal{G}(E_c; w_0) \frac{2ww_0(A_0 - 2A_1 - A_3) + 2(3w_0^2 + ww_3 - 2w_0w_3)(A_1 - A_0)}{w_1^2w_0^4w_2^2} \\
& + \mathcal{G}(E_c; w_3) \left[\frac{2w(3ww_0 - 4ww_3 - 5w_0w_3 + 6w_3^2)(-A_1 + A_2 - 2A_3)}{3(w - w_3)^3w_2^2w_3^4} \right. \\
& \left. + \frac{2(w - 3w_3)(w + 2w_0 - 3w_3)(A_1 - A_0)}{3(w - w_3)^3w_2^2w_3^3} \right]. \tag{B4h}
\end{aligned}$$

3. $W_j^{(4)}$

All terms proportional to Δ^4 can be written as $W_j^{(4)} = \mathcal{W}_j^{(4)} A_0$, with all quantity $\mathcal{W}_j^{(4)}$ giving by

$$\mathcal{W}_1^{(4)} = -\frac{1}{E_c^5} \frac{3}{2}, \tag{B5a}$$

$$\mathcal{W}_3^{(4)}(w_0) = -\frac{1}{E_c^5} \frac{1}{2w_0} - \frac{1}{E_c^3} \frac{2}{w_0^3} - \frac{1}{E_c} \frac{8}{w_0^5} + \mathcal{H}(E_c; w_0) \frac{8}{w_0^5}, \tag{B5b}$$

$$\mathcal{W}_5^{(4)}(w) = \frac{1}{E_c^5} \frac{3}{2w} + \frac{1}{E_c^3} \frac{2}{w^3} - \frac{1}{E_c} \frac{8}{w^5} + \mathcal{I}(E_c; w) \frac{8}{w^4} + \mathcal{H}(E_c; w) \frac{8}{w^5}, \tag{B5c}$$

$$\begin{aligned}
\mathcal{W}_7^{(4)}(w, w_0) = & \frac{1}{E_c^5} \frac{1}{2ww_0} + \frac{1}{E_c^3} \frac{2(w^2 - w_0^2)}{w^3w_0^3} + \frac{1}{E_c} \frac{8(w^4 - w^2w_0^2 - 2ww_0^3 - 3w_0^4)}{w^5w_0^5} \\
& - \mathcal{I}(E_c; w) \frac{8}{w^4w_1} - \mathcal{H}(E_c; w) \frac{8(w + 3w_1)}{w^5w_1^2} - \mathcal{H}(E_c; w_0) \frac{8(w - 2w_0)}{w_1^2w_0^5}. \tag{B5d}
\end{aligned}$$

$$\mathcal{W}_2^{(4)}(w_3) = -\frac{1}{E_c^5} \frac{1}{10w_3} - \frac{1}{E_c^3} \frac{2}{3w_3^3} - \frac{1}{E_c} \frac{8}{w_3^5} + \mathcal{G}(E_c; w_3) \frac{8}{w_3^6}, \quad (\text{B5e})$$

$$\begin{aligned} \mathcal{W}_4^{(4)}(w_0, w_3) = & -\frac{1}{E_c^5} \frac{3}{10w_0w_3} - \frac{1}{E_c^3} \frac{2(3w_0^2 + 2w_0w_3 + w_3^2)}{3w_0^3w_3^3} - \frac{1}{E_c} \frac{8(3w_0^4 + 2w_0^3w_3 + w_0^2w_3^2 - w_3^4)}{w_0^5w_3^5} \\ & - \mathcal{H}(E_c; w_0) \frac{8}{w_0^5w_2} + \mathcal{G}(E_c; w_0) \frac{8(3w_0 - 2w_3)}{w_0^6w_2^2} + \mathcal{G}(E_c; w_3) \frac{8(3w_0 - 4w_3)}{w_2^2w_3^6}, \quad (\text{B5f}) \end{aligned}$$

$$\begin{aligned} \mathcal{W}_6^{(4)}(w, w_3) = & \frac{1}{E_c^5} \frac{1}{10ww_3} + \frac{1}{E_c^3} \frac{2(w^2 + w_3^2)}{3w^3w_3^3} + \frac{1}{E_c} \frac{8(w^4 + w^2w_3^2 + w_3^4)}{w^5w_3^3} \\ & + \mathcal{G}(E_c; w) \frac{8w_3}{w^6(w^2 - w_3^2)} - \mathcal{G}(E_c; w_3) \frac{8w}{w_3^6(w^2 - w_3^2)}, \quad (\text{B5g}) \end{aligned}$$

and

$$\begin{aligned} \mathcal{W}_8^{(4)}(w, w_0, w_3) = & \frac{1}{E_c^5} \frac{3}{10ww_0w_3} + \frac{1}{E_c^3} \frac{2[w^2(3w_0^2 + 2w_0w_3 + w_3^2) - w_0^2w_3^2]}{3w^3w_0^3w_3^3} \\ & + \frac{1}{E_c} \frac{8((3w_0^4 + 2w_3w_0^3 + w_3^2w_0^2 - w_3^4)w^4 + (w_3^2 - w_0^2)w^2w_0^2w_3^2 + w_0^3w_3^4(2w + 3w_0))}{w^5w_0^5w_3^5} \\ & + \mathcal{I}(E_c; w) \frac{8}{w^4w_1(w - w_3)} + \mathcal{H}(E_c; w) \frac{8(8w^2 - 7ww_0 - 6ww_3 + 5w_0w_3)}{w^5w_1^2(w - w_3)^2} \\ & - \mathcal{G}(E_c; w) \frac{8[18w^3 - 8w_0w_3^2 + ww_3(21w_0 + 10w_3) - w^2(15w_0 + 26w_3)]}{w^6w_1^2(w - w_3)^3} \\ & + \mathcal{H}(E_c; w_0) \frac{8(w - 2w_0)}{(w - w_0)^2w_0^5(w_0 - w_3)} - \mathcal{G}(E_c; w_0) \frac{8(w - 2w_0)(3w_0 - 2w_3)}{(w - w_0)^2w_0^6(w_0 - w_3)^2} \\ & + \mathcal{G}(E_c; w_3) \frac{8[(4w_3 - 3w_0)w^2 + 3(3w_0 - 4w_3)w_3w + 2w_3^2(5w_3 - 4w_0)]}{(w - w_3)^3(w_0 - w_3)^2w_3^6}. \quad (\text{B5h}) \end{aligned}$$

REFERENCES

- ¹F. Bonaccorso, Z. Sun, T. Hasan, and A. C. Ferrari, *Nat. Photon.* **4**, 611 (2010).
- ²T. Low and P. Avouris, *ACS Nano* **8**, 1086 (2014).
- ³K. J. A. Ooi and D. T. H. Tan, *Proc. R. Soc. A* **473**, 20170433 (2017).
- ⁴Z. Sun, A. Martinez, and F. Wang, *Nat. Photon.* **10**, 227 (2016).
- ⁵A. Autere, H. Jussila, Y. Dai, Y. Wang, H. Lipsanen, and Z. Sun, *Adv. Mater.* **30**, 1705963 (2018).
- ⁶N. Yoshikawa, T. Tamaya, and K. Tanaka, *Science* **356**, 736 (2017).
- ⁷M. Baudisch, A. Marini, J. D. Cox, T. Zhu, F. Silva, S. Teichmann, M. Massicotte, F. Koppens, L. S. Levitov, F. J. G. de Abajo, and J. Biegert, *Nat. Commun.* **8**, 1018 (2018).
- ⁸D. Dimitrovski, L. B. Madsen, and T. G. Pedersen, *Phys. Rev. B* **95**, 035405 (2017).

- ⁹M. Taucer, T. J. Hammond, P. B. Corkum, G. Vampa, C. Couture, N. Thiré, B. E. Schmidt, F. Légaré, H. Selvi, N. Unsuree, B. Hamilton, T. J. Echtermeyer, and M. A. Denecke, *Phys. Rev. B* **96**, 195420 (2017).
- ¹⁰R. W. Boyd, *Nonlinear Optics*, 3rd ed. (Academic, 2008).
- ¹¹C. Aversa and J. E. Sipe, *Phys. Rev. B* **52**, 14636 (1995).
- ¹²M. Zhao, Z. Ye, R. Suzuki, Y. Ye, H. Zhu, J. Xiao, Y. Wang, Y. Iwasa, and X. Zhang, *Light Sci. App.* **5**, e16131 (2016).
- ¹³D. B. S. Soh, C. Rogers, D. J. Gray, E. Chatterjee, and H. Mabuchi, *Phys. Rev. B* **97**, 165111 (2018).
- ¹⁴A. Y. Bykov, T. V. Murzina, M. G. Rybin, and E. D. Obraztsova, *Phys. Rev. B* **85**, 121413 (2012).
- ¹⁵Y. Q. An, F. Nelson, J. U. Lee, and A. C. Diebold, *Nano Lett.* **13**, 2104 (2013).
- ¹⁶Y. Q. An, J. E. Rowe, D. B. Dougherty, J. U. Lee, and A. C. Diebold, *Phys. Rev. B* **89**, 115310 (2014).
- ¹⁷M. Glazov and S. Ganichev, *Phys. Rep.* **535**, 101 (2014).
- ¹⁸H. Yu, D. Talukdar, W. Xu, J. B. Khurgin, and Q. Xiong, *Nano Lett.* **15**, 5653 (2015).
- ¹⁹J. L. Cheng, N. Vermeulen, and J. E. Sipe, *Opt. Express* **22**, 15868 (2014).
- ²⁰S. Wu, L. Mao, A. M. Jones, W. Yao, C. Zhang, and X. Xu, *Nano Lett.* **12**, 2032 (2012).
- ²¹J. B. Khurgin, *Appl. Phys. Lett.* **67**, 1113 (1995).
- ²²H. M. van Driel and J. E. Sipe, in *Encyclopedia of Modern Optics*, edited by B. Guenther (Elsevier, Oxford, 2005) pp. 137 – 143.
- ²³H. M. van Driel and J. E. Sipe, in *Ultrafast Phenomena in Semiconductors*, edited by K.-T. Tsen (Springer, New York, 2001) pp. 261–306.
- ²⁴J. Rioux and J. Sipe, *Physica E* **45**, 1 (2012).
- ²⁵D. Sun, C. Divin, J. Rioux, J. E. Sipe, C. Berger, W. A. de Heer, P. N. First, and T. B. Norris, *Nano Lett.* **10**, 1293 (2010).
- ²⁶D. Sun, J. Rioux, J. E. Sipe, Y. Zou, M. T. Mihnev, C. Berger, W. A. de Heer, P. N. First, and T. B. Norris, *Phys. Rev. B* **85**, 165427 (2012).
- ²⁷J. Rioux, G. Burkard, and J. E. Sipe, *Phys. Rev. B* **83**, 195406 (2011).
- ²⁸C. Salazar, J. L. Cheng, and J. E. Sipe, *Phys. Rev. B* **93**, 075442 (2016).
- ²⁹R. A. Muniz and J. E. Sipe, *Phys. Rev. B* **91**, 085404 (2015).
- ³⁰K. M. Rao and J. E. Sipe, *Phys. Rev. B* **86**, 115427 (2012).

- ³¹J. Rioux, J. E. Sipe, and G. Burkard, Phys. Rev. B **90**, 115424 (2014).
- ³²B. M. Fregoso, R. A. Muniz, and J. E. Sipe, Phys. Rev. Lett. **121**, 176604 (2018).
- ³³B. M. Fregoso, “Bulk photovoltaic effects in the presence of a static electric field,” (2018), arXiv:1806.01206.
- ³⁴G. Xing, H. Guo, X. Zhang, T. C. Sum, and C. H. A. Huan, Opt. Express **18**, 4564 (2010).
- ³⁵R. Wu, Y. Zhang, S. Yan, F. Bian, W. Wang, X. Bai, X. Lu, J. Zhao, and E. Wang, Nano Lett. **11**, 5159 (2011).
- ³⁶H. Yang, X. Feng, Q. Wang, H. Huang, W. Chen, A. T. S. Wee, and W. Ji, Nano Lett. **11**, 2622 (2011).
- ³⁷H. Zhang, S. Virally, Q. Bao, L. K. Ping, S. Massar, N. Godbout, and P. Kockaert, Opt. Lett. **37**, 1856 (2012).
- ³⁸T. Gu, N. Petrone, J. F. McMillan, A. van der Zande, M. Yu, G. Q. Lo, D. L. Kwong, J. Hone, and C. W. Wong, Nat. Photon. **6**, 554 (2012).
- ³⁹N. Vermeulen, D. Castelló-Lurbe, J. L. Cheng, I. Pasternak, A. Krajewska, T. Ciuk, W. Strupinski, H. Thienpont, and J. Van Erps, Phys. Rev. Appl. **6**, 044006 (2016).
- ⁴⁰E. Dremetsika, B. Dlubak, S.-P. Gorza, C. Ciret, M.-B. Martin, S. Hofmann, P. Seneor, D. Dolfi, S. Massar, P. Emplit, and et al., Opt. Lett. **41**, 3281 (2016).
- ⁴¹T. Jiang, D. Huang, J. Cheng, X. Fan, Z. Zhang, Y. Shan, Y. Yi, Y. Dai, L. Shi, K. Liu, C. Zeng, J. Zi, J. E. Sipe, Y.-R. Shen, W.-T. Liu, and S. Wu, Nat. Photon. **12**, 430 (2018).
- ⁴²N. Vermeulen, D. Castelló-Lurbe, M. Khoder, I. Pasternak, A. Krajewska, T. Ciuk, W. Strupinski, J. Cheng, H. Thienpont, and J. V. Erps, Nat. Comm. **9**, 2675 (2018).
- ⁴³R. Binder, ed., Optical Properties of Graphene (World Scientific Publishing, 2016).
- ⁴⁴J. L. Cheng, N. Vermeulen, and J. E. Sipe, Phys. Rev. B **91**, 235320 (2015); **93**, 039904 (2016).
- ⁴⁵J. L. Cheng, N. Vermeulen, and J. E. Sipe, Phys. Rev. B **92**, 235307 (2015).
- ⁴⁶V. Margulis, E. Muryumin, and E. Gaiduk, Solid State Commun. **246**, 76 (2016).
- ⁴⁷J. L. Cheng, N. Vermeulen, and J. E. Sipe, New J. Phys. **16**, 053014 (2014); **18**, 029501 (2016).